Egypt. J. Chem. **Vol. 67** No. 3 pp. 495 - 513 (2024)

Egyptian Journal of Chemistry

http://ejchem.journals.ekb.eg/

One-pot Three-Component Synthesis, *In vitro* Anticancer Activity and p53-MDM2 Protein-Protein Interaction Inhibition of Novel Spiro-Oxindoline-Based Pyrazolo[3,4-*b*]Pyridines

Dana M. Odeh[1], Heba Abdelrasheed Allam[1]*, Walaa R. Mahmoud[1], Mohanad M. Odeh[2], Hatem A. Abdel-Aziz[3], Eman R. Mohammed[1]

[1]Department of Pharmaceutical Chemistry, Faculty of Pharmacy, Cairo University, Kasr El-Aini Street, Cairo, P.O. Box, 11562, Egypt

[2] Department of Clinical Pharmacy and Pharmacy Practice, Faculty of Pharmaceutical Sciences, The Hashemite University, P.O. Box 330127, Zarqa 13133, Jordan

[3]Department of Applied Organic Chemistry, National Research Center, Dokki, Cairo 12622, Egypt

Abstract

Two series of spiro-indoline-pyrazolo[3,4-b]pyridines 6a-f and 7a-f were synthesized via a one-pot three-component reaction of indoline-2,3-diones, 3-oxo-3-arylpropanenitriles and 1,3-diphenyl-1H-pyrazol-5-amine. Preliminary anti-cancer activity evaluation of 6a-f and 7a-f on 60 cancer cell lines was performed at the (NCI/USA). Compounds 7b-f were selected by the NCI for 5-dose assay, revealing very promising activity against almost the full panel with GI50 range 6.05-49.70, 14.60-53.20, 2.99-38.70, 2.47-16.80 and 3.40-20.70 µM, respectively, and GI50 (MG-MID) Full panel = 18.11, 22.93, 13.19, 6.04, 12.20 µM, respectively. The inhibitory activity of p53-MDM2 protein-protein interaction for 7b-f in MCF7 cell line showed that 7f was the most potent compound with IC50 = 3.05 ± 0.12 µM and 2.7-folds increase in activity when compared with nutlin-1 (IC50 = 8.21 ± 0.25 µM). Furthermore, compound 7b increased the level of p53 and p21 by 3.86- and 1.78-folds in leukemia MOLT4 cancer cell line, similarly 7e and 7f increased the level of p53 by 2.53- and 2.98-folds, respectively, whereas p21 increased by 2.74- and 2.43-folds in cancer cells of non-small cell lung cancer HOP92, respectively. Compounds 7b, 7e and 7f induced a significant level of early and late apoptosis on MCF7. Compounds 7b-f revealed good binding mode in the cleft of p53 on MDM2 in their molecular docking studies.

Keywords: Spiro-indolines, pyrazolo[3,4-b]pyridines, anticancer, p53-MDM2, apoptosis.

1-Introduction

Cancer is a lethal disease that is considered to be one of the major causes of death globally with a relatively large population share in developing countries in cancer-related deaths. The early future will see an exhausting global load due to the ongoing annual increase in cancer cases. [1]. The conventional anticancer chemotherapeutics showed serious side effects including damage of the immune system in addition to their toxicity and inefficiency because of their nonspecific targeting [2]. Small molecule inhibitors are the main category of targeted drugs designed to interfere with the specific genes or proteins necessary for tumor growth and progression, accordingly, most of the newly approved anticancer drugs are small molecule targeted anticancer agents [3].

On the other side, protein–protein interactions (PPIs) are responsible for important biological processes such as cell growth and differentiation, intracellular signaling and programmed cell death (apoptosis) [4]. P53 is a tumor suppressor protein that plays a critical role in the management of cell cycle, apoptosis and DNA repair [5]. Due to its role in preventing genome alterations and the growth of tumors, it has been referred to as "the guardian of the genome." [6]. The protein identified as murine double minute 2 (MDM2) is an essential negative regulator of p53 [7].

*Corresponding author e-mail heba.abdelkhalek@pharma.cu.edu.eg; (Heba Abdelrasheed Allam)
Receive Date: 11 August 2023 Revise Date: 19 August 2023 Accept Date: 30 August 2023
DOI: 10.21608/EJCHEM.2023.228742.8415

MDM2 (HDM2 in human) is an inhibitor of p53, it inhibits p53 function through p53–MDM2 interaction which is mediated by hydrophobic surface pocket in MDM2 and three key hydrophobic amino acid residues in p53, namely Phe19, Trp23, and Leu26 [8]. This inhibition affects the expression of genes involved in apoptosis, DNA repair, and cell cycle arrest and could lead to rapid and impressive regression of tumors [9]. Small-molecule inhibitors, which block the p53-MDM2 interaction, may be effective in the treatment of human cancer by reactivating the p53 tumor suppressor function [10-13]. The successful design and development of small-molecule inhibitors of the p53-MDM2 interaction led to the introduction of a considerable number of such compounds into human clinical trials as novel anticancer medications [14-18].

Cis-diphenyl substituted imidazolines (Nutlins) were identified as the first class of potent, specific inhibitors of the p53-MDM2 interaction [8, 19]. Nutlin-3a (Rebemadlin) is a potent MDM2 inhibitor and p53 protein stabilizer that induces cell autophagy and apoptosis [10]. It is a potential therapeutic agent for the treatment of TP53 wild-type ovarian carcinomas with IC_{50} = 4.0-6.0 μM [20] (Figure 1). RG7112 (Figure 1) was the first MDM2 inhibitor that entered clinical evaluation [21] and was conducted in patients with hematological malignancies, including acute lymphoblastic leukemia (ALL) [22, 23]. Furthermore, a potent MDM2 inhibitor; RG7388 (Figure 1), also known as Idasanutlin, has been identified and was included in a cutting-edge study for the treatment of tumors, including acute myeloid leukaemia. (AML) [24]. Additionally, RG7388 potently inhibited tumors by activating p53 pathway in nasopharyngeal carcinoma (NPC) [25] and it explored a pre-clinical efficacy in the treatment of ovarian cancer [26]

Spiro-oxindoles are a class of potential p53-MDM2 inhibitors that has been progressively developed and many of them have gained regulatory approval over the last years [1, 8, 11, 13, 14, 18, 27]. For example, RO8994 (Figure 1) is identified as highly potent and selective p53-MDM2 inhibitor, and it represents a new generation of p53–MDM2 antagonists with marked improvement in both *in vitro* and *in vivo* pharmacological properties for potential clinical development [28]. MI-1061 (Figure 1) is a potent, orally bioavailable MDM2 inhibitor (IC_{50} = 4.4 nM, K_i = 0.16 nM), that revealed excellent chemical stability, and achieved tumor regression in the SJSA-1 xenograft tumor model in mice [29]. Additionally, MI-63 has shown strong binding affinity (K_i=3 nM) for MDM2 with pronounced effects on pediatric cancer cells [30] whereas, MI-219 selectively inhibited the growth of wild-type (wt) p53-containing lung cancer cells by induction of G1 or G2 arrest [31] (Figure 1).

Furthermore, the MDM2 inhibitor MI-77301 (SAR405838) (Figure 1) was evaluated as potent and specific p53-MDM2 interaction inhibitor, which has been involved into clinical development, for its therapeutic potential in the treatment of endocrine-resistant breast cancer [32]. In addition, MI-888 (Figure 1) was identified as potent MDM2 inhibitor (K_i = 0.44 nM) with a superior pharmacokinetic profile and enhanced *in vivo* efficacy. It achieved rapid, complete, and durable tumor regression in two types of xenograft models of human cancers [33].

Interestingly, the spiro-oxindole derivative (**Ia**) showed potent and broad spectrum of anticancer activity toward NCI full panel with GI_{50} (MG-MID) = 3.97 μM, it also induced apoptosis in MCF-7 and MDA-MB-231 cancer cell lines. Moreover, compounds (**Ia**) and (**Ib**) inhibited p53-MDM2 protein–protein interaction with IC_{50} = 52.1 and 95.2 nM, respectively [34] (Figure 1). In addition, spiro-oxindoles **IIa-c** revealed potential anti-proliferative activity against TNBC MDA-MB-231 cells with IC_{50} = 6.70, 6.40 and 6.70 mM, respectively. Furthermore, compounds (**IIb**) and (**IIc**) induced apoptosis in MDA-MB-231 cells through the up-regulation of the Bax and down-regulation of the Bcl-2, besides boosting caspase-3 levels, It is worthy to mention that these derivatives were chosen as an important template for designing new target compounds [35] (Figure 1).

In the light of the previous findings and as a continuation of our research program on the development of novel spiro-oxindole derivatives as potential anticancer agents [34, 35], we aim in the present investigation to synthesize two novel series of spiro-oxindoles **6a-f** and **7a-f** (Figure 1) to evaluate their anticancer activity against NCI 60 cancer cell lines. In addition, the potential apoptotic induction and their effects on cell cycle progression will be investigated. Furthermore, the most potent spiro-oxindoles will be assayed for their potential inhibitory activity towards p53-MDM2 protein–protein interaction.

2. Experimental

2.1. Chemistry

The data of the devices used in the analytical experiments in the chemistry sector were pronounced in the supplementary file.

*2.1.1. Synthesis of 1-methylindoline-2,3-dione (**2a**) and 1-benzylindoline-2,3-dione (**2b**).*

To a mixture of indoline-2,3-dione (1.47 g, 10 mmol) and methyl iodide (1.70 g, 12 mmol) or benzyl chloride (1.52 g, 12 mmol) in DMF (30 mL), anhydrous K_2CO_3 (4.14 g, 30 mmol) was added. The

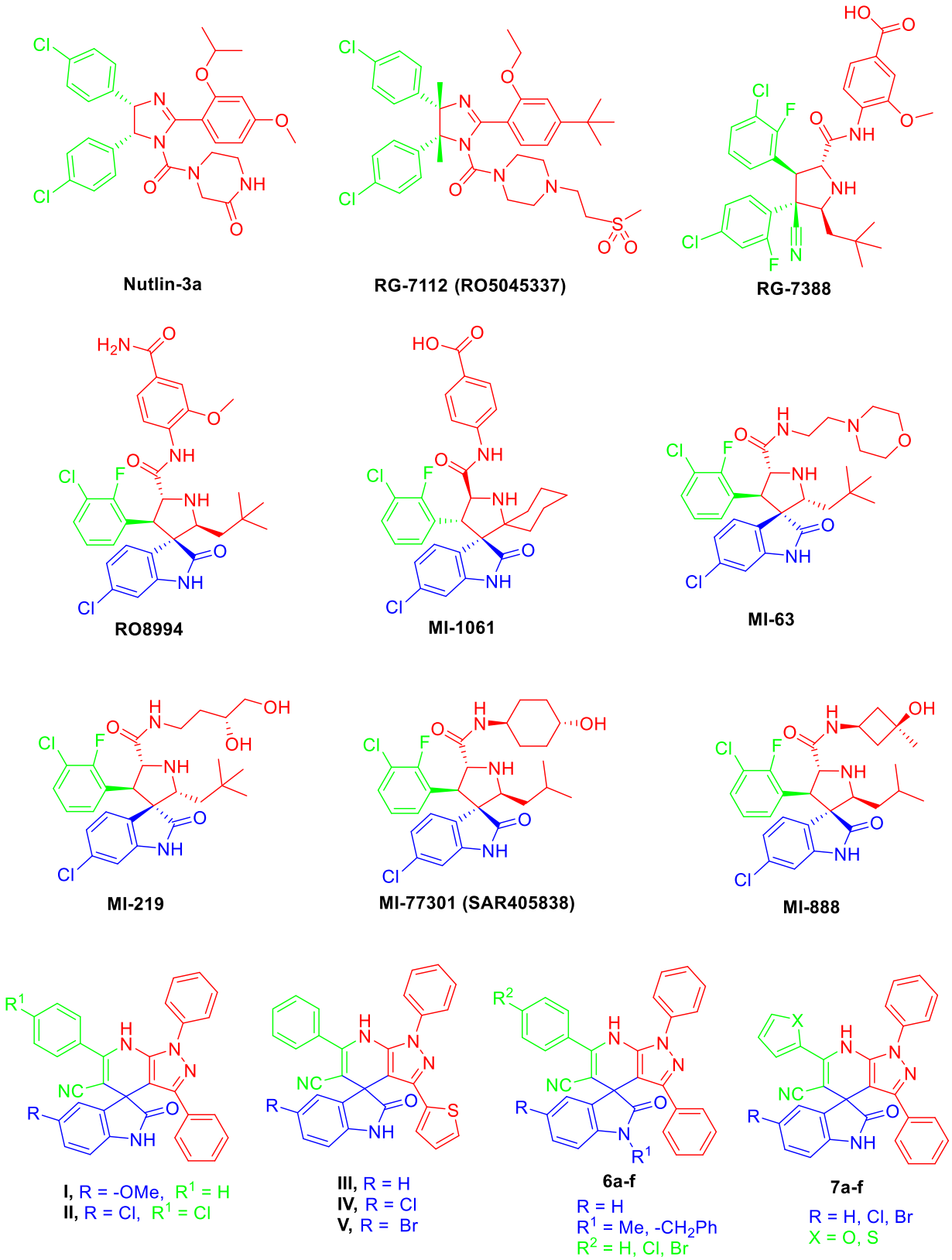

Figure 1. Structure of highly potent anticancer agents and inhibitors of the p53-MDM2; imidazolines, spiro-oxindoles and the targeted spiro-oxindoles **6a-f** and **7a-f**.

mixture was stirred at room temperature for 4 and 12 hrs, respectively, then was poured into ice. The formed precipitate was filtered, washed with water and crystallized from EtOH to afford the corresponding 1-methylindoline-2,3-dione (**2a**) and 1-benzylindoline-2,3-dione (**2b**), in 80 and 82% yield and m.p. 129-130ºC and 131ºC, respectively [36, 37].

*2.1.2. Synthesis of 3-oxo-3-arylpropanenitrile **4a-e**.*

A mixture of the appropriate ethyl esters **3a-e** (10 mmol), acetonitrile (0.52 mL, 10 mmol), and sodium hydride (0.46 g, 10 mmol, 60%) in dry toluene (30 mL) was refluxed for 12 h, allowed to cool to room temperature. The formed solid was filtered, washed with ether and dried. The obtained solid was dissolved in water and the obtained solution was neutralized with concentrated hydrochloric acid to pH 7. The product was filtered, washed with water and then dried. Crystallization from ethanol afforded 3-oxo-3-arylpropanenitrile **4a-e**. Physical properties of **4a-e** were identical to those reported in the literature [38]; 3-Oxo-3-phenylpropanenitrile (**4a**), 66% yield and m.p. 75-76ºC; 3-oxo-3-(*p*-tolyl)propanenitrile (**4b**), 61% yield and m.p. 100-101ºC; 3-(4-chlorophenyl)-3-oxopropanenitrile (**4c**), 70% yield and m.p. 125-126ºC; 3-(furan-2-yl)-3-oxopropanenitrile (**4d**), 60% yield and m.p. 66-68ºC; 3-oxo-3-(thiophen-2-yl)propanenitrile (**4e**) 56% yield and m.p. 123-126ºC.

*2.1.3. Synthesis of 1,3-diphenyl-1H-pyrazol-5-amine (**5**)*

A mixture of 3-oxo-3-phenylpropanenitrile (**1a**) (1.45 g, 10 mmol) and phenyl hydrazine (0.98 mL, 10 mmol) was fused and heated for 15 min. The reaction mixture was then cooled and triturated with ethanol. The crystalline product was filtered and washed with ethanol. Recrystallization from ethanol afforded the desired 1,3-diphenyl-1*H*-pyrazol-5-amine (**5**) in 85% yield. M.p.130-132 ºC (reported 129-131ºC) [39].

*2.1.4. Synthesis of 1-(methyl/benzyl)-2-oxo-1',3'-diphenyl-6'-(aryl)-1',7'-dihydrospiro[indoline-3,4'-pyrazolo[3,4-b]pyridine]-5'-carbonitrile **6a-f**.*

A mixture of 1-methylindoline-2,3-dione (**2a**) (0.16 g, 1 mmol) or 1-benzylindoline-2,3-dione (**2b**) (0.24 g, 1 mmol), the appropriate 3-oxo-3-arylpropanenitrile derivatives **2a-c** (1 mmol) and 1,3-diphenyl-1*H*-pyrazol-5-amine (0.24 g, 1 mmol) (**5**) in AcOH/H_2O (v/v = 1:1, 20 mL) was refluxed for 4 h. The obtained precipitate, upon cooling was filtered, washed with water and recrystallized from AcOH to afford compounds **6a-f**, respectively.

*2.1.4.1. 1-Methyl-2-oxo-1',3',6'-triphenyl-1',7'-dihydrospiro[indoline-3,4'-pyrazolo[3,4-b]pyridine]-5'-carbonitrile (**6a**)*

Orange powder, 46% yield; mp >300ºC; IR (KBr) ν_{max}/cm^{-1} 3250 (NH), 2212 (C≡N), 1695 (C=O), 1626 (C=N); ^{1}H NMR (DMSO-d_6, 400 MHz) δ 2.95 (s, 3H, -NCH_3), 6.81 (d, *J* = 6.8 Hz, 2H, Ar H), 6.93 (d, *J* = 9.6 Hz, 1H, Ar H), 7.07-7.19 (m, 3H, Ar H), 7.24-7.37 (m, 3H, Ar H), 7.43-7.47 (m, 2H, Ar H), 7.53-7.61 (m, 5H, Ar H), 7.65-7.67 (m, 2H, Ar H), 7.74 (d, *J* = 7.6 Hz, 1H, Ar H), 10.52 (s, D_2O exchangeable, 1H, NH pyridine); ^{13}C NMR (DMSO-d_6, 100 MHz) δ 26.60 (N-$\underline{C}H_3$), 51.40 (C4 pyridine), 82.63 (-$\underline{C}$-C≡N), 98.90 (C4 pyrazole), 109.10 (-C-$\underline{C}$≡N), 118.78, 123.80, 124.43 (2C), 125.26, 125.35, 128.16 (2C), 128.18 (2C), 128.52, 128.91 (2C), 129.39 (2C), 129.84 (2C), 131.01, 132.76, 133.86, 135.24, 138.32, 138.80, 140.95, 142.70, 148.98, 152.25, 176.70 (C=O); MS *m/z* (%) 505.53 (M$^+$, 7.08), 338.73 (100); Anal. Calcd. For: $C_{33}H_{23}N_5O$ (505.58): C, 78.40; H, 4.59; N, 13.85; Found: C, 78.63; H, 4.70; N, 14.09.

*2.1.4.2. 1-Methyl-2-oxo-1',3'-diphenyl-6'-(p-tolyl)-1',7'-dihydrospiro[indoline-3,4'-pyrazolo[3,4-b]pyridine]-5'-carbonitrile (**6b**)*

Orange powder, 63% yield; mp >300ºC; IR (KBr) ν_{max}/cm^{-1} 3260 (NH), 2201 (C≡N), 1697 (C=O), 1609 (C=N); ^{1}H NMR (DMSO-d_6, 400 MHz) δ 2.40 (s, 3H, -CH_3), 2.96 (s, 3H, -NCH_3), 6.79-6.93 (m, 3H, Ar H), 7.09-7.18 (m, 3H, Ar H), 7.23-7.34 (m, 5H, Ar H), 7.43-7.60 (m, 5H, Ar H), 7.72-7.74 (m, 2H, Ar H), 10.41 (s, D_2O exchangeable, 1H, NH pyridine); ^{13}C NMR (DMSO-d_6, 100 MHz) δ 21.38 (-$\underline{C}H_3$), 26.56 (N-$\underline{C}H_3$), 51.37 (C4 pyridine), 82.23 (-$\underline{C}$-C≡N), 98.90 (C4 pyrazole), 109.07 (-C-$\underline{C}$≡N), 118.91, 122.88, 123.81, 124.34 (2C), 125.20 (2C), 128.12 (2C), 128.17 (2C), 128.53, 129.25 (2C), 129.41 (2C), 129.85 (2C), 130.94, 132.70, 135.23, 138.28, 138.82, 140.94, 142.66, 148.95, 152.27, 176.75 (C=O); MS *m/z* (%) 519.97 (M$^+$, 29.81), 77.31 (100); Anal. Calcd. For: $C_{34}H_{25}N_5O$ (519.61): C, 78.59; H, 4.85; N, 13.48; Found: C, 78.37; H, 4.66; N, 13.71.

*2.1.4.3. 6'-(4-Chlorophenyl)-1-methyl-2-oxo-1',3'-diphenyl-1',7'-dihydrospiro[indoline-3,4'-pyrazolo[3,4-b]pyridine]-5'-carbonitrile (**6c**)*

Orange powder, 50% yield; mp; 290-292ºC; IR (KBr) ν_{max}/cm^{-1} 3284 (NH), 2203 (C≡N), 1698 (C=O), 1611 (C=N); ^{1}H NMR (DMSO-d_6, 400 MHz) δ 2.93 (s, 3H, -NCH_3), 6.76-6.93 (m, 3H, Ar H), 7.01-7.17 (m, 3H, Ar H), 7.22-7.47 (m, 4H, Ar H), 7.55-7.74 (m, 8H, Ar H), 10.50 (s, D_2O exchangeable, 1H, NH pyridine); ^{13}C NMR (DMSO-d_6, 100 MHz) δ 26.57 (N-$\underline{C}H_3$), 51.30 (C4 pyridine), 82.83 (-$\underline{C}$-C≡N), 98.80 (C4 pyrazole), 109.12 (-C-

C≡N), 118.56, 123.85, 124.42 (2C), 125.29, 128.11 (2C), 128.19 (2C), 128.27, 128.57 (2C), 128.99 (2C), 129.90 (2C), 131.33 (2C), 132.55, 132.60, 135.07, 135.76, 138.12, 138.59, 142.60, 148.97, 151.21, 176.62 (C=O); MS *m/z* (%) 540.61 (M^+, 17.43), 244.11 (100); Anal. Calcd. For: $C_{33}H_{22}ClN_5O$ (540.02): C, 73.40; H, 4.11; N, 12.97; Found: C, 73.64; H, 4.29; N, 13.18.

*2.1.4.4. 1-Benzyl-2-oxo-1',3',6'-triphenyl-1',7'-dihydrospiro[indoline-3,4'-pyrazolo[3,4-b]pyridine]-5'-carbonitrile (**6d**)*

Orange powder, 59% yield; mp 288-290ºC; IR (KBr) ν_{max}/cm^{-1} 3280 (NH), 2199 (C≡N), 1687 (C=O), 1610 (C=N); ^{1}H NMR (DMSO-d_6, 400 MHz) δ 4.45 (d, J = 15.6 Hz, 1H of -CH_2-), 4.90 (d, J = 20.4 Hz, 1H of -CH_2-), 6.72-6.81 (m, 3H, Ar H), 7.06-7.80 (m, 3H, Ar H), 7.20-7.31 (m, 6H, Ar H), 7.37-7.38 (m, 1H, Ar H), 7.40-7.47 (m, 1H, Ar H), 7.54-7.60 (m, 6H, Ar H), 7.65-7.67 (m, 2H, Ar H), 7.74-7.75 (m, 2H, Ar H), 10.52 (s, D_2O exchangeable, 1H, NH pyridine); ^{13}C NMR (DMSO-d_6, 100 MHz) δ 43.90 (-CH_2-), 51.46 (C4 pyridine), 82.64 (-C-C≡N), 98.55 (C4 pyrazole), 109.72 (-C-C≡N), 119.07, 123.93, 124.46 (2C), 125.51, 127.67 (2C), 127.80 (2C), 128.17 (2C), 128.22, 128.59 (2C), 128.92 (2C), 128.97 (2C), 129.39 (2C), 129.72, 129.86 (2C), 131.05, 132.63, 133.80, 135.07, 135.99, 138.25, 138.93, 142.09, 149.02, 152.41, 177.03 (C=O); MS *m/z* (%) 581.72 (M^+, 19.07), 574.78 (100); Anal. Calcd. For: $C_{39}H_{27}N_5O$ (581.68): C, 80.53; H, 4.68; N, 12.04; Found: C, 80.29; H, 4.76; N, 12.31.

*2.1.4.5. 1-Benzyl-2-oxo-1',3'-diphenyl-6'-(p-tolyl)-1',7'-dihydrospiro[indoline-3,4'-pyrazolo[3,4-b]pyridine]-5'-carbonitrile (**6e**)*

Orange crystals, 62% yield; mp >300ºC; IR (KBr) ν_{max}/cm^{-1} 3250 (NH), 2200 (C≡N), 1701 (C=O), 1606 (C=N); ^{1}H NMR (DMSO-d_6, 400 MHz) δ 2.38 (s, 1H, CH_3), 4.46 (d, J = 16.0 Hz, 1H of -CH_2-), 4.92 (d, J = 16.0 Hz, 1H of -CH_2-), 6.73 (d, J = 7.6 Hz, 1H, ArH), 6.73 (d, J = 7.2 Hz, 2H, ArH), 7.06-7.16 (m, 3H, Ar H), 7.20-7.23 (m, 2H, Ar H), 7.26-7.30 (m, 3H, Ar H), 7.32-7.37 (m, 5H, Ar H), 7.45 (t, J = 7.2 Hz, 1H, Ar H), 7.56-7.60 (m, 4H, Ar H), 7.75 (d, J = 7.6 Hz, 2H, Ar H), 10.47 (s, D_2O exchangeable, 1H, NH pyridine); ^{13}C NMR (DMSO-d_6, 100 MHz) δ 21.42 (-CH_3), 43.92 (-CH_2-), 51.48 (C4 pyridine), 82.31 (-C-C≡N), 98.63 (C4 pyrazole), 109.72 (-C-C≡N), 119.22, 123.92, 124.40 (2C), 125.48, 127.68 (2C), 127.81 (2C), 128.18 (2C), 128.22, 128.58 (2C), 128.99 (2C), 129.31 (2C), 129.42 (2C), 129.69, 129.86 (2C), 130.97, 132.68, 135.13, 136.01, 138.30, 139.01, 140.96, 142.12, 149.03, 142.42, 177.08 (C=O); MS *m/z* (%) 595.12 (M^+, 28.90), 591.22 (100); Anal. Calcd. For: $C_{40}H_{29}N_5O$ (595.71): C, 80.65; H, 4.91; N, 11.76; Found: C, 80.47; H, 5.08; N, 11.94.

*2.1.4.6. 1-Benzyl-6'-(4-chlorophenyl)-2-oxo-1',3'-diphenyl-1',7'-dihydrospiro[indoline-3,4'-pyrazolo[3,4-b]pyridine]-5'-carbonitrile (**6f**)*

Orange powder, 38% yield; mp >300ºC; IR (KBr) ν_{max}/cm^{-1} 3260 (NH), 2209 (C≡N), 1650 (C=O), 1563 (C=N); ^{1}H NMR (DMSO-d_6, 400 MHz) δ 4.46 (d, J = 20.4 Hz, 1H of -CH_2-), 4.91 (d, J = 20.4 Hz, 1H of -CH_2-), 6.73 (d, J = 7.6 Hz, 1H, ArH), 6.80 (d, J = 8.0 Hz, 2H, ArH), 7.06-7.10 (m, 3H, Ar H), 7.20-7.32 (m, 7H, Ar H), 7.39 (d, J = 7.2 Hz, 1H, Ar H), 7.46 (t, J = 6.0 Hz, 1H, Ar H), 7.56-7.62 (m, 4H, Ar H), 7.68-7.75 (m, 4H, Ar H), 10.55 (s, D_2O exchangeable, 1H, NH pyridine); MS *m/z* (%) 616.07 (M^+, 52.19), 176.51 (100); Anal. Calcd. For: $C_{39}H_{26}ClN_5O$ (616.12): C, 76.03; H, 4.25; N, 11.37; Found: C, 76.24; H, 4.39; N, 11.54.

*2.1.4. Synthesis of 5-(substituted)-6'-(furan/thiophene-2-yl)-2-oxo-1',3'-diphenyl-1',7'-dihydrospiro[indoline-3,4'-pyrazolo[3,4-b]pyridine]-5'-carbonitrile **7a-f**.*

These derivatives were synthesized by the same method adopted for the preparation of compounds **6a-f** using indoline-2,3-diones **1a-c**, 3-oxo-3-(furan-2-yl/thiophen-2-yl)propanenitrile derivatives **2d, e** and 1,3-diphenyl-1*H*-pyrazol-5-amine (**5**) in AcOH/H_2O (v/v = 1:1, 20 mL).

*2.1.5.1. 6'-(Furan-2-yl)-2-oxo-1',3'-diphenyl-1',7'-dihydrospiro[indoline-3,4'-pyrazolo[3,4-b]pyridine]-5'-carbonitrile (**7a**)*

Pale yellow powder, 68% yield; mp 292-294ºC; IR (KBr) ν_{max}/cm^{-1} 3233 (2NH), 2201 (C≡N), 1714 (C=O), 1622 (C=N); ^{1}H NMR (DMSO-d_6, 400 MHz) δ 6.73-6.79 (m, 2H, ArH), 6.88 (d, J = 6.4 Hz, 2H, ArH), 7.00 (t, J = 7.2 Hz, 1H, ArH), 7.11-7.25 (m, 6H, Ar H), 7.39 (t, J = 6.8 Hz, 1H, Ar H), 7.62 (t, J = 7.2 Hz, 2H, Ar H), 7.74 (d, J = 8.4 Hz, 1H, Ar H), 7.99 (s, 1H, Ar H), 10.15 (s, D_2O exchangeable, 1H, NH indoline), 10.55 (s, D_2O exchangeable, 1H, NH pyridine); ^{13}C NMR (DMSO-d_6, 100 MHz) δ 51.66 (C4 pyridine), 81.45 (-C-C≡N), 98.72 (C4 pyrazole), 110.32 (-C-C≡N), 112.65, 114.87, 118.39, 123.12, 123.78 (2C), 125.57, 128.11 (2C), 128.21 (2C), 128.54, 129.85 (2C), 130.01 (2C), 132.76, 135.60, 138.54, 140.41, 141.70, 145.29, 145.70, 147.43, 148.95, 178.16 (C=O); MS *m/z* (%) 481.46 (M^+, 33.21), 270.47 (100); Anal. Calcd. For: $C_{30}H_{19}N_5O_2$ (481.52): C, 74.83; H, 3.98; N, 14.54; Found: C, 74.61; H, 4.15; N, 14.68.

*2.1.5.2. 5-Chloro-6'-(furan-2-yl)-2-oxo-1',3'-diphenyl-1',7'-dihydrospiro[indoline-3,4'-pyrazolo[3,4-b]pyridine]-5'-carbonitrile (**7b**)*

Pale yellow powder, 75% yield; mp 299-301ºC; IR (KBr) ν_{max}/cm^{-1} 3300-3102 (2NH), 2205 (C≡N), 1709 (C=O), 1621 (C=N); ^{1}H NMR (DMSO-d_6, 400 MHz) δ 6.74-6.78 (m, 2H, ArH), 6.92 (d, *J* = 7.2 Hz, 2H, ArH), 7.51-7.20 (m, 3H, ArH), 7.24-7.33 (m, 3H, Ar H), 7.48 (t, *J* = 7.2 Hz, 1H, Ar H), 7.62 (t, *J* = 7.2 Hz, 2H, Ar H), 7.74 (d, *J* = 9.2 Hz, 2H, Ar H), 7.99 (s, 1H, Ar H), 10.22 (s, D_2O exchangeable, 1H, NH indoline), 10.71 (s, D_2O exchangeable, 1H, NH pyridine); MS *m/z* (%) 515.73 (M^+, 30.35), 276.32 (100); Anal. Calcd. For: $C_{30}H_{18}ClN_5O_2$ (515.96): C, 69.84; H, 3.52; N, 13.57; Found: C, 69.62; H, 3.70; N, 13.75.

*2.1.5.3. 5-Bromo-6'-(furan-2-yl)-2-oxo-1',3'-diphenyl-1',7'-dihydrospiro[indoline-3,4'-pyrazolo[3,4-b]pyridine]-5'-carbonitrile (**7c**)*

Pale yellow powder, 65% yield; mp 301-303ºC; IR (KBr) ν_{max}/cm^{-1} 3251 (2NH), 2206 (C≡N), 1718 (C=O), 1626 (C=N); ^{1}H NMR (DMSO-d_6, 400 MHz) δ 6.73-6.75 (m, 2H, ArH), 6.94 (d, *J* = 6.4 Hz, 2H, ArH), 7.16-7.29 (m, 4H, ArH), 7.40-7.50 (m, 3H, Ar H), 7.62 (t, *J* = 8.0 Hz, 2H, Ar H), 7.76 (t, *J* = 7.6 Hz, 2H, Ar H), 8.0 (s, 1H, Ar H), 10.20 (s, D_2O exchangeable, 1H, NH indoline), 10.70 (s, D_2O exchangeable, 1H, NH pyridine); ^{13}C NMR (DMSO-d_6, 100 MHz) δ 51.78 (C4 pyridine), 80.45 (-C-C≡N), 98.18 (C4 pyrazole), 112.23 (-C-C≡N), 112.69, 114.67, 115.08, 118.36, 123.96 (2C), 128.08 (2C), 128.18 (2C), 128.34 (2C), 128.42, 128.69, 129.99 (2C), 132.66, 137.63, 138.49, 138.62, 140.73, 141.03, 145.15, 145.79, 148.87, 177.92 (C=O); MS *m/z* (%) 560.05 (M^+, 25.64), 90.95 (100); Anal. Calcd. For: $C_{30}H_{18}BrN_5O_2$ (560.41): C, 64.30; H, 3.24; N, 12.50; Found: C, 64.49; H, 3.51; N, 12.68.

*2.1.5.4. 2-Oxo-1',3'-diphenyl-6'-(thiophen-2-yl)-1',7'-dihydrospiro[indoline-3,4'-pyrazolo[3,4-b]pyridine]-5'-carbonitrile (**7d**)*

Pale yellow powder, 74% yield; mp 295-297ºC; IR (KBr) ν_{max}/cm^{-1} 3200 (2NH), 2208 (C≡N), 1708 (C=O), 1634 (C=N); ^{1}H NMR (DMSO-d_6, 400 MHz) δ 6.78 (d, *J* = 5.6 Hz, 1H, ArH), 6.88 (d, *J* = 6.8 Hz, 2H, ArH), 7.01 (t, *J* = 7.6 Hz, 1H, ArH), 7.13 (t, *J* = 7.6 Hz, 2H, ArH), 7.22-7.24 (m, 4H, ArH), 7.46 (t, *J* = 7.2 Hz, 1H, ArH), 7.58-7.62 (m, 3H, ArH), 7.74 (d, *J* = 6.8 Hz, 2H, Ar H), 7.86 (d, *J* = 5.6 Hz, 1H, Ar H), 10.34 (s, D_2O exchangeable, 1H, NH indoline), 10.54 (s, D_2O exchangeable, 1H, NH pyridine); MS *m/z* (%) 497.50 (M^+, 45.86), 99.58 (100); Anal. Calcd. For: $C_{30}H_{19}N_5OS$ (497.58): C, 72.42; H, 3.85; N, 14.08; Found: C, 72.31; H, 3.98; N, 14.29.

*2.1.5.5. 5-Chloro-2-oxo-1',3'-diphenyl-6'-(thiophen-2-yl)-1',7'-dihydrospiro[indoline-3,4'-pyrazolo[3,4-b]pyridine]-5'-carbonitrile (**7e**)*

Pale yellow powder, 60% yield; mp 297-299ºC; IR (KBr) ν_{max}/cm^{-1} 3250-3105 (2NH), 2200 (C≡N), 1697 (C=O), 1615(C=N); ^{1}H NMR (DMSO-d_6, 400 MHz) δ 6.78 (d, *J* = 8.0 Hz, 1H, ArH), 6.93 (d, *J* = 8.0 Hz, 2H, ArH), 7.16-7.35 (m, 6H, ArH), 7.47 (t, *J* = 7.2 Hz, 1H, ArH), 7.58-7.64 (m, 3H, ArH), 7.75 (d, *J* = 7.2 Hz, 2H, ArH), 7.86 (dd, *J* = 5.2, 1.2 Hz, 1H, Ar H), 10.40 (s, D_2O exchangeable, 1H, NH indoline), 10.70 (s, D_2O exchangeable, 1H, NH pyridine); ^{13}C NMR (DMSO-d_6, 100 MHz) δ 52.13 (C4 pyridine), 82.58 (-C-C≡N), 98.45 (C4 pyrazole), 111.79 (-C-C≡N), 118.55, 123.99 (2C), 125.67, 127.03, 128.06 (2C), 128.13 (2C), 128.33, 128.66 (2C), 129.78 (2C), 129.88, 130.24, 131.26, 132.69, 133.96, 137.22, 138.42, 138.99, 140.58, 145.23, 148.81, 178.01 (C=O); MS *m/z* (%) 532.12 (M^+, 48.67), 515.51 (100); Anal. Calcd. For: $C_{30}H_{18}ClN_5OS$ (532.02): C, 67.73; H, 3.41; N, 13.16; Found: C, 67.90; H, 3.66; N, 13.42.

*2.1.5.6. 5-Bromo-2-oxo-1',3'-diphenyl-6'-(thiophen-2-yl)-1',7'-dihydrospiro[indoline-3,4'-pyrazolo[3,4-b]pyridine]-5'-carbonitrile (**7f**)*

Pale yellow powder, 68% yield; mp 293-295ºC; IR (KBr) ν_{max}/cm^{-1} 3259 (2NH), 2206 (C≡N), 1717 (C=O), 1650(C=N); ^{1}H NMR (DMSO-d_6, 400 MHz) δ 6.75 (d, *J* = 5.6 Hz, 1H, ArH), 6.95 (d, *J* = 5.2 Hz, 2H, ArH), 7.19-7.28 (m, 4H, ArH), 7.40-7.47 (m, 3H, ArH), 7.59-7.64 (m, 3H, ArH), 7.75-7.77 (m, 2H, ArH), 7.86-7.87 (m, 1H, ArH), 10.47 (s, D_2O exchangeable, 1H, NH indoline), 10.73 (s, D_2O exchangeable, 1H, NH pyridine); MS *m/z* (%) 576.00 (M^+, 36.99), 460.83 (100); Anal. Calcd. For: $C_{30}H_{18}BrN_5OS$ (576.47): C, 62.51; H, 3.15; N, 12.15; Found: C, 62.78; H, 3.37; N, 12.41.

2.2. Biological Evaluation

2.2.1. In vitro anticancer NCI screening at single and five dose concentrations.

The preliminary cytotoxicity study for the synthesized compounds was determined as described in the protocol of the National Cancer Institute (NCI), Bethesda, USA against a panel of 60 cell lines using sulforhodamine B (SRB) protein assay [40] and then cell viability and growth was determined, as previously described [41, 42]. Five doses screening depends on the same principle of the one-dose screening, but the desired final maximum concentration of the test compound was prepared, and the additional four concentrations were prepared as 10-fold or ½ log serial dilutions of the desired final maximum test concentration (0.01, 0.1, 1, 10, 100 µM).

2.2.2. MTT assay for cytotoxicity:

Standard MTT colorimetric assay was applied to test the IC_{50} of the tested compounds against WI-38 normal renal cell line with the typical

reported methodology of MTT colorimetric assay [43].

2.2.3. In vitro inhibitory activity for 7b-f on p53-MDM2 protein-protein interaction

The inhibitory activity of compounds 7b-f on p53-MDM2 protein-protein interaction was assessed in MCF7 cell line using nutlin-1 as reference compound, the detailed procedure was explained in the supplementary.

*2.2.4. Effect of compounds **7b-f** on p53* in HepG2

Please refer to supplementary data.

*4.2.5. Effect of compounds **7b**, **7e** and **7f** on the level of p21 and p53 in MOLT4 and HOP92 cells*

MOLT4 and HOP92 cells were treated with compounds **7b**, **7e** and **7f** at their IC_{50} concentrations, and the level of p21 and p53 was measured using ELISA colorimetric kits (abcam Human p21 ELISA Kit, catalog number ab136945 and p53 ELISA Human Kit, product number CS0070 (Sigma), according to the manufacturer's instructions, as reported earlier [34].

2.2.6. Apoptotic assay

Apoptosis study of the most active compounds was accomplished using the Annexin V-FITC Apoptosis Detection Kit (K101-25, BioVision®, Mountain View, Canada) at their IC_{50} concentration values on the specified cell after 24 h in three successive steps; according to the manufacturer's instructions and according to the reported procedure [44, 45].

2.2.7. Molecular docking study

All the molecular modeling studies were carried out using Molecular Operating Environment (MOE, 2019.0102) software. All minimizations were performed with MOE until an RMSD gradient of 0.1 kcal·mol^{-1}Å^{-1} with MMFF94x force field and the partial charges were automatically calculated. The X-ray crystallographic structure of MDM2 was downloaded from the protein data bank with PDB ID of 3LBL. For each co-crystallized enzyme, water molecules and ligands which are not involved in the binding were removed, the protein was prepared for the docking study using *Protonate 3D* protocol in MOE with default options. The co-crystalized ligands were used to define the binding site for docking. Triangle Matcher placement method and London dG scoring function were used for docking [46].

3-Results and Discussion

3.1. Chemistry

The one-pot three components synthesis of spiro-indoline-pyrazolo[3,4-*b*]pyridines **6a-f** is based on the reaction of three reported starting materials; 1-(methyl/benzyl)indoline-2,3-diones **2a**,**b** [36, 37], 3-oxo-3-arylpropanenitriles **4a-c** [38] and 1,3-diphenyl-1*H*-pyrazol-5-amine **5** [39] in refluxing AcOH/H_2O (1:1 v/v) (Scheme 1). The structures of **6a-f** were in full agreement with their spectral and elemental analyses data for example, the ^{1}H NMR spectra of **6a-f** revealed a D_2O-exchangeable singlet signal due to pyridine NH proton at range δ 10.42-10.55 ppm. In addition, singlet signals of the methyl protons of compounds **6a-c** were appeared in the range δ 2.93-3.96 ppm, whereas the methylene protons of compounds **6d-f** appeared as two doublet signals, each one integer to one proton, around δ 4.45-4.46 and 4.90-4.92 ppm with J = 15.6-20.4 Hz. Moreover, ^{13}C NMR spectra of **6a-f** showed signals of carbon of the carbonyl group around δ 177.0 ppm, whereas the signals of the carbons of the methyl groups of **6a-c** and signals of the carbon of the methylene group of **6d-f** appeared around δ 26.5 and 43.9 ppm, respectively. IR spectra of **6a-f** exhibited the absorption bands of the pyridine NH group in the region 3250-3284 cm^{-1}, absorption band of C≡N in the region 2199-2212 cm^{-1} and the band of C=O group in the region 1650-1701 cm^{-1}.

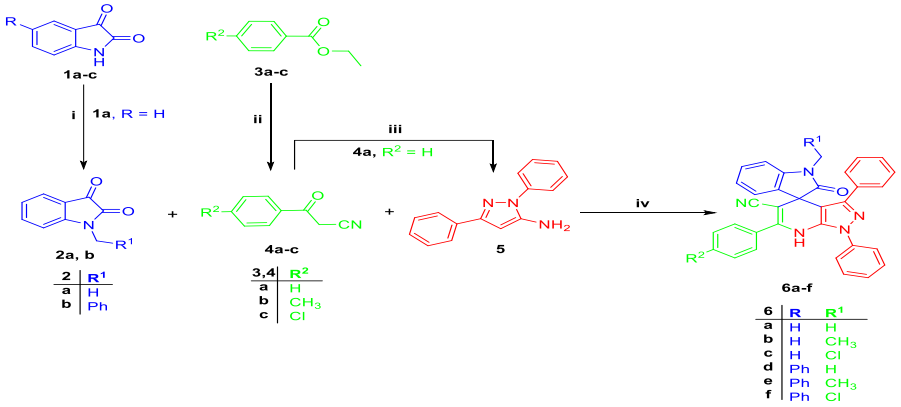

Scheme 1. Reagents and conditions; (**i**). Methyl iodide or benzyl chloride, DMF, K_2CO_3, stirring at rt for 4 and 12 h, respectively; (**ii**). CH_3CN, DMF, NaH, toluene, reflux 12 h; (**iii**). Phenylhydrazine, neat, reflux 15 min; (**iv**) AcOH/H_2O (1:1 v/v), reflux 4 h.

The proposed synthetic routes (A, B and C) for the synthesis of compounds **6a-f** are illustrated in Figure 2. Route A showed that 1-(methyl/benzyl)indoline-2,3-diones **2a**, **b** reacted first with 3-oxo-3-arylpropanenitriles **4a-c** to give intermediate **1A** which then reacted with 1,3-diphenyl-1*H*-pyrazol-5-amine **5** to give intermediate **1C** and finally the corresponding spiro-indoline-pyrazolo[3,4-*b*]pyridines **6a-f** [47].

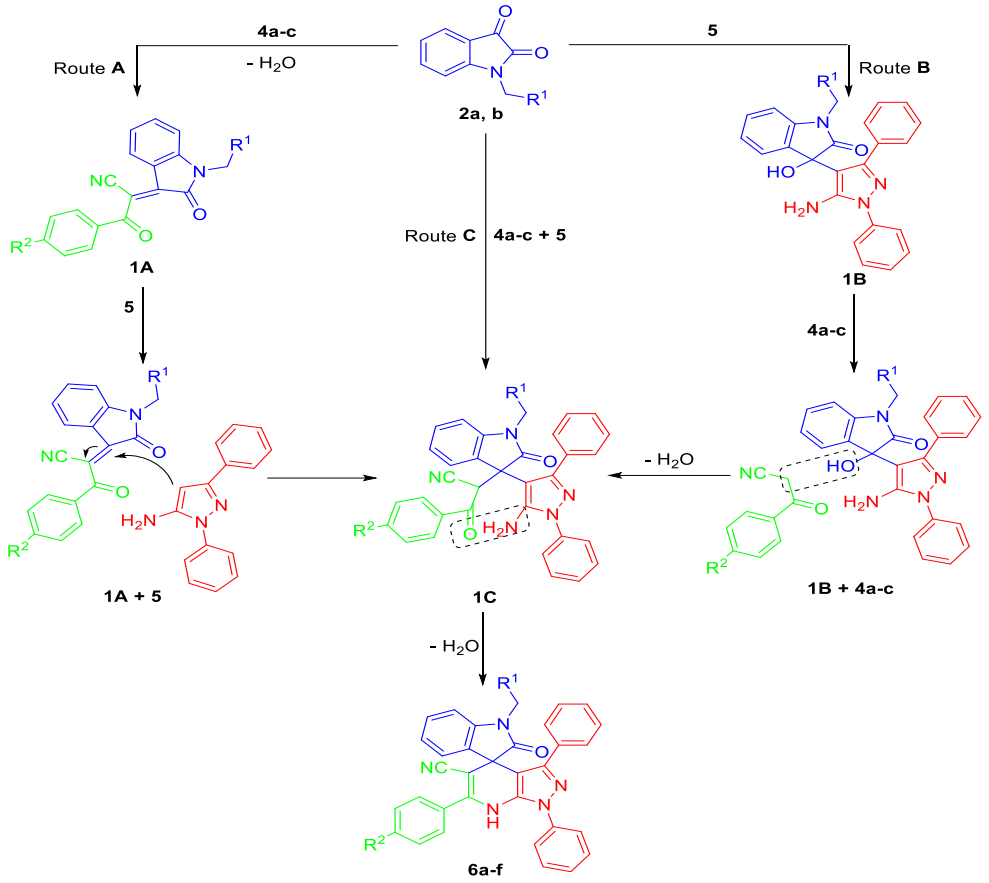

Figure 2. The proposed mechanism pathways (Routes A, B and C) for the synthesis of the target compounds **6a-f**.

On the other hand, route **B** proposed that the reaction proceeded through the initial reaction between 1-(methyl/benzyl)indoline-2,3-diones **2a**, **b** and 1,3-diphenyl-1*H*-pyrazol-5-amine **5** to give intermediate **1B** which was reacted with 3-oxo-3-arylpropanenitriles **4a-c** to afford intermediate **1C** and finally **6a-f** [48]. However, the latter pathways **A** and **B** (Figure 1) gave practically low yields when compared with the three-component one-pot reaction (Route C) [34].

the IR spectra of **7a-f** showed the absorption bands of the indoline and pyridine NH groups in the region 3102-3300 cm^{-1} and the characteristic sharp absorption band of C≡N in the region 2201-2208 cm^{-1} in addition to the carbonyl absorption band in the region 1697-1718 cm^{-1}.

Similarly, the target spiro-indoline-pyrazolo[3,4-*b*]pyridines **7a-f** were prepared by one-pot three-component reaction of indoline-2,3-diones **1a-c**, 3-oxo-3-(furan-2-yl/thiophen-2-yl)propanenitrile derivatives **4d,e** that were prepared from the corresponding ethyl esters **3d,e** and 1,3-diphenyl-1*H*-pyrazol-5-amine **5** in AcOH/H_2O (v/v = 1:1) (Scheme 2). The ^{1}H NMR spectra of **7a-f** revealed two D_2O-exchangeable singlet signals of indoline and pyridine NH protons at range δ 10.15-10.47 and 10.54-10.74 ppm, respectively. In addition,

3.2. Biological evolution

3.2.1. One dose in vitro anti-cancer activity against full NCI 60 cell lines

To evaluate the anti-cancer activity against a panel of NCI 60 cancer cell lines, the 12 newly

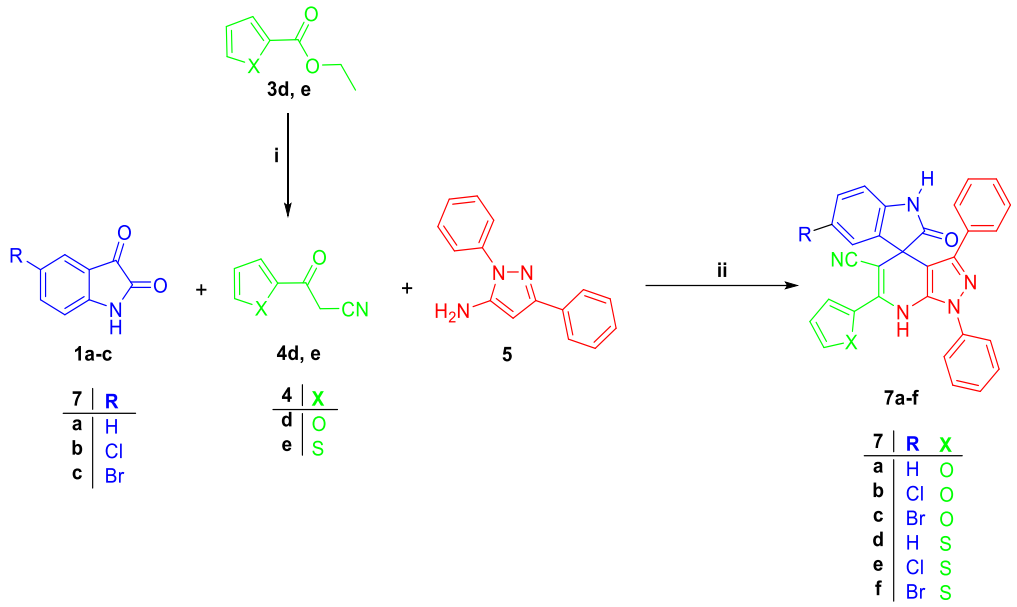

Scheme 2. Reagents and conditions; (**i**). CH_3CN, DMF, NaH, toluene, reflux 12 h; (**iv**) $AcOH/H_2O$ (2:1 v/v), reflux 4 h.

synthesized spiro-oxindoline-pyrazolo[3,4-*b*]pyridines **6a-f**, and **7a-f** were submitted to the National Cancer Institute (NCI) Developmental Therapeutic Program (www.dtp.nci.nih.gov). The latter compounds were screened at 10 µM against full panel 60 cancer cell lines, which contains nine subpanel cancer types: leukemia, melanoma, lung, colon, CNS, ovarian, renal, prostate and breast cancers and their data are expressed as percentages of growth inhibition (GI %) (Supporting data). Six compounds; **6a-f** showed weak or moderate activity. Compound **7a** showed moderate activity with an exceptional effect on the cancer cell line SNB-75 (GI % = 86.09). Surprisingly, five compounds, **7b-f** revealed superior activity with GI % = 80.70-99.94 while, compounds **7c**, **7d** and **7e** showed broad spectrum anticancer activity against 57, 52 and 54 cell lines with significant GI% ≥ 80.00% for 7, 26 HOP-62 and NCI-H460 (GI % = 98.50, 89.51 and 98.84, respectively), colon cancer cells HCT-116 (GI% = 94.92), CNS cancer cells U251 (GI% = 98.15), renal cancer cells SN12C (GI% = 94.89) and finally against breast cancer cells HS 578T (GI% = 93.99) (Table 1). Compound **7d** showed selective activity against three subpanels namely; (1): leukemia cells (5 cell lines from 6, 83.33%) with GI% = 93.98, 99.30, 90.34, 84.95 and 98.54% for CCRF-CEM, HL-60(TB), K-562, MOLT-4 and SR cells, respectively; (2): non-small cell lung carcinoma (NSCLC) (6 cell lines from 9, 66.67%) with GI% = 94.58, 85.16, 87.16, 86.43, 94.42 and 94.31% for A549/ATCC, EKVX, NCI-H226, NCI-H23, NCI-H460 and NCI-H522 cells, respectively; (3): colon cancer cells (5 and 24 cell lines, respectively. On the other hand, compounds **7b** and **7f** exhibited activity against 41 and 20 cell lines with significant GI% ≥ 80.00% for 11 and 17 cell lines, respectively (Table 1).

Compound **7b** showed high GI% against leukemia cell line K-562 (GI % = 90.15), non-small cell lung carcinoma (NSCLC) cell lines NCI-H460 and NCI-H522 (GI % = 99.84 and 99.94, respectively), colon cancer cells SW-620 (GI % = 84.12), CNS cancer cells SF-268, SF-295 and SNB-19 (GI % = 88.98, 93.09 and 96.78, respectively), melanoma cancer cells LOX IMVI cells (GI % = 97.45), ovarian cancer cells OVCAR-4 (GI % = 90.06), renal cancer cells ACHN (GI % = 91.06) and breast cancer cells BT-549 (GI % = 84.59). Compound **7c** showed pronounced GI on non-small cell lung carcinoma (NSCLC) cells A549/ATCC,

cell lines from 7, 71.43%) with GI% = 94.47, 88.14, 93.33, 90.97 and 91.26% for HCT-116, HCT-15, HT29, KM12 and SW-620 cells, respectively (Table 1). Compound **7e** exhibited selective activity against subpanel leukemia cells (5 cell lines from 6, 83.33%) with GI% = 86.30, 88.86, 80.70, 86.86 and 87.40% for CCRF-CEM, K-562, MOLT-4, RPMI-8226 and SR cells, respectively. It also showed growth inhibition against non-small cell lung carcinoma (NSCLC) with GI% = 86.67, 93.83 and 96.62% for EKVX, NCI-H460 and NCI-H522 cells, respectively (Table 1). Compound **7d** also exhibited selective activity against subpanel colon cancer cells (4 cell lines from 7, 57.14%) with GI% = 88.51, 89.55, 85.64 and 84.65% for HCT-116, HCT-15, HT29 and

Table 1. NCI 60 cell lines *in vitro* screening (one-dose, concentration 10μM) for compounds **7a-f** in %GI.

Cell line/Compound	7a	7b	7c	7d	7e	7f
Leukemia						
CCRF-CEM	59.41	75.00	64.48	93.98	86.30	98.14
HL-60(TB)	32.07	56.21	48.93	99.30	L	L
K-562	56.59	90.15	78.84	90.34	88.86	97.25
MOLT-4	38.33	65.22	63.81	84.95	80.70	L
RPMI-8226	39.85	50.16	52.21	65.53	86.68	97.15
SR	48.80	L	68.07	98.54	87.40	L
Non-Small Cell Lung Cancer						
A549/ATCC	39.04	L	98.50	94.58	75.65	L
EKVX	30.10	75.85	43.80	85.16	86.67	92.58
HOP-62	40.27	L	89.51	L	71.20	L
HOP-92	52.49	L	47.62	L	L	L
NCI-H226	26.93	L	32.76	87.16	48.4	87.03
NCI-H23	9.72	54.37	29.43	86.43	76.18	97.82
NCI-H322M	4.63	49.34	13.11	19.91	52.91	73.11
NCI-H460	47.30	99.84	98.84	94.42	93.83	L
NCI-H522	48.89	99.94	68.24	94.31	96.62	L
Colon Cancer						
COLO 205	4.78	20.40	13.11	44.06	L	L
HCC-2998	--	35.22	8.23	61.89	73.94	93.72
HCT-116	62.74	L	94.92	94.47	88.51	L
HCT-15	39.17	69.65	61.39	88.14	89.55	L
HT29	28.70	58.05	50.53	93.33	85.64	L
KM12	14.49	47.86	33.59	90.97	84.65	L
SW-620	11.18	84.12	53.66	91.26	78.7	L
CNS Cancer						
SF-268	23.11	88.98	50.94	45.72	76.78	84.34
SF-295	25.53	93.09	27.46	59.66	87.14	L
SF-539	22.62	L	L	L	79.53	L
SNB-19	14.12	96.78	39.97	74.56	86.63	92.01
SNB-75	86.09	L	L	39.48	63.12	L
U251	34.66	L	98.15	88.41	83.8	L
Melanoma						
LOX IMVI	30.09	97.45	78.65	38.36	74.22	L
MALME-3M	10.30	77.67	09.25	73.15	23.72	L
M14	24.15	77.56	57.99	85.41	83.53	L
MDA-MB-435	10.44	46.29	40.22	71.69	58.78	L
SK-MEL	--	19.78	12.98	9.91	77.2	L
SK-MEL-28	15.27	54.41	32.52	84.8	58.17	L
SK-MEL-5	28.55	49.62	41.01	76.12	74.89	99.63
UACC-257	--	43.61	26.90	12.04	36.47	64.23
UACC-62	16.76	62.57	48.48	51.51	84.65	L
Ovarian Cancer						
IGROV1	2.79	60.75	32.99	49.34	75.97	L
OVCAR-3	--	L	57.55	87.28	76.91	L
OVCAR-4	29.92	90.06	58.41	70.81	72.75	99.35
OVCAR-5	7.52	46.53	25.13	42.31	94.97	L
OVCAR-8	31.75	L	75.02	75.77	71.98	L
NCI/ADR-RES	30.17	L	70.08	38.36	66.97	89.49
SK-OV-3	39.07	44.68	20.00	71.57	41.00	L
Renal Cancer						
786-0	19.18	L	56.55	98.75	77.73	L
A498	--	--	--	L	11.19	L
ACHN	39.02	91.06	50.65	L	87.44	L
CAKI-1	24.14	67.01	44.12	36.59	76.74	90.36
RXF 393	66.25	42.11	29.83	L	L	L
SN12C	27.40	L	94.89	44.72	66.24	L
TK-10	21.71	L	34.15	81.93	68.51	87.89
UO-31	32.64	56.92	40.22	81.84	87.35	93.62
Prostate Cancer						
PC-3	41.54	L	75.9	93.02	87.23	L
DU-145	13.06	57.65	29.53	66.46	49.50	68.54
Breast Cancer						
MCF7	41.35	78.71	60.21	68.62	84.88	92.77
MDA-MB-231/ATCC	42.01	L	66.77	65.78	78.45	L
HS 578T	65.11	L	93.99	95.41	91.85	L
BT-549	--	84.59	29.56	L	L	L
T-47D	37.14	73.43	51.53	82.66	88.96	98.19
MDA-MB-468	23.80	57.72	33.38	L	L	L

%GI = percentage of Growth Inhibition, %GI ≥80% is blue highlighted; L= The compound is “Lethal”.

Table 2. Five dose NCI *in vitro* testing for compounds **7b-f** (GI_{50}, TGI, and LC_{50} in μM).

Cell line/Compound	GI_{50} (μM)					TGI (μM)					LC50 (μM)				
	7b	7c	7d	7e	7f	7b	7c	7d	7e	7f	7b	7c	7d	7e	7f
Leukemia															
CCRF-CEM	49.7	---	7.52	3.35	7.51	>100	---	46.8	20.7	26.7	>100	---	>100	>100	84.3
HL-60(TB)	15.0	53.2	5.75	3.51	8.84	>100	>100	45.6	11.7	66.8	>100	>100	>100	>100	74.8
K-562	16.6	38.0	6.17	4.46	7.53	>100	>100	38.9	34.1	23.6	>100	>100	>100	>100	65.3
MOLT-4	6.05	35.2	12.0	4.95	7.92	91.2	>100	41.1	23.4	24.1	>100	>100	>100	>100	63.9
RPMI-8226	18.7	35.9	8.60	4.30	10.2	>100	>100	83.7	27.5	32.9	>100	>100	>100	>100	>100
SR	23.3	48.9	12.7	4.93	7.93	>100	>100	58.1	36.3	27.1	>100	>100	>100	>100	79.8
Non-Small Cell Lung Cancer															
A549/ATCC	11.6	17.4	10.2	4.12	10.2	25.1	33.0	23.0	15.9	23.0	54.3	62.9	52.1	45.8	52.2
EKVX	16.5	20.9	11.2	4.33	11.1	66.0	54.6	33.9	18.0	27.4	>100	>100	>100	50.3	67.7
HOP-62	14.8	18.4	17.0	7.02	15.4	28.9	37.8	44.1	21.4	29.6	56.2	77.6	>100	51.4	56.6
HOP-92	12.8	16.8	3.52	2.47	3.40	28.6	33.2	15.0	7.94	15.4	63.8	65.4	78.9	38.6	52.4
NCI-H226	17.5	21.1	16.9	11.6	15.4	50.2	44.4	42.5	28.2	31.2	>100	93.6	>100	68.4	63.5
NCI-H23	15.5	21.5	12.9	5.57	9.98	3.24	47.7	31.8	18.2	21.8	67.5	>100	78.5	47.6	47.6
NCI-H322M	35.4	43.3	38.7	13.0	19.4	>100	>100	>100	31.1	47.6	>100	>100	>100	74.1	>100
NCI-H460	14.1	17.9	11.3	4.07	11.2	31.8	33.4	24.1	14.1	24.6	71.8	62.2	51.5	44.2	54.0
NCI-H522	14.5	20.4	2.99	2.60	4.52	38.8	48.4	15.8	9.87	17.1	>100	>100	79.2	35.2	41.5
Colon Cancer															
COLO 205	14.7	25.4	15.5	14.3	16.0	29.7	69.1	34.9	29.5	29.9	60.0	>100	78.7	60.7	56.0
HCC-2998	19.2	36.5	14.0	7.13	13.9	58.9	>100	35.6	19.8	27.0	>100	>100	90.8	45.6	52.5
HCT-116	13.1	18.6	11.9	3.95	12.1	26.0	36.3	28.1	16.3	24.7	51.4	70.9	66.4	60.1	50.5
HCT-15	19.6	18.1	8.92	3.74	5.34	>100	36.9	24.0	14.1	18.2	>100	75.2	60.1	41.8	43.5
HT29	14.7	18.3	14.0	4.82	15.2	30.2	35.2	28.3	17.1	29.1	62.3	68.1	57.0	42.4	55.8
KM12	49.5	33.2	5.13	3.65	7.67	>100	>100	20.4	13.6	20.5	>100	>100	67.3	40.7	47.0
SW-620	30.3	30.0	9.57	4.56	11.1	>100	97.6	28.6	16.6	26.5	>100	>100	83.5	47.3	62.8
CNS Cancer															
SF-268	17.8	26.8	18.9	3.52	8.58	90.1	74.0	>100	19.0	37.8	>100	>100	>100	92.4	>100
SF-295	16.9	19.6	12.8	3.74	12.5	56.3	50.0	33.3	15.9	25.6	>100	>100	86.1	41.6	52.6
SF-539	17.9	18.1	15.2	4.77	15.2	40.6	35.1	31.7	17.0	28.5	91.9	68.3	66.1	41.4	53.6
SNB-19	17.4	18.6	9.25	3.12	5.23	46.0	42.2	>100	14.2	27.9	>100	95.7	>100	58.8	>100
SNB-75	---	16.0	8.48	2.60	---	---	38.0	30.8	13.0	---	---	90.1	98.7	38.0	---
U251	13.3	18.0	6.23	3.88	5.64	29.2	33.4	20.6	14.4	18.4	64.1	62.1	52.1	40.3	45.6
Melanoma															
LOX IMVI	19.2	18.1	14.4	6.46	12.4	47.1	34.8	32.4	20.4	24.9	>100	67.0	72.8	50.6	49.9
MALME-3M	14.7	16.1	15.9	14.3	14.5	29.8	2.99	30.0	27.4	27.8	60.1	55.4	56.5	52.6	53.3
M14	15.0	18.5	15.0	4.94	14.4	32.7	36.8	32.7	18.4	27.7	71.5	73.2	71.1	49.0	53.4
MDA-MB-435	34.8	24.2	17.8	11.1	17.0	>100	61.5	37.2	23.9	33.7	>100	>100	78.0	51.4	66.9
SK-MEL	---	18.1	15.8	3.97	---	---	36.6	38.3	14.6	---	---	74.2	93.1	38.9	---
SK-MEL-28	15.5	17.9	14.9	11.1	15.1	33.0	33.6	29.3	23.2	28.4	70.1	62.8	57.5	48.5	53.5
SK-MEL-5	18.0	18.0	13.7	10.8	16.5	41.8	32.6	29.4	23.1	30.5	97.0	59.0	63.2	49.7	56.1
UACC-257	16.6	20.5	18.1	12.9	15.6	41.4	50.6	48.3	25.8	30.9	>100	>100	>100	51.5	61.3
UACC-62	11.4	17.2	13.7	4.13	11.4	28.2	32.1	27.9	16.9	23.6	69.4	59.8	56.9	41.7	48.8
Ovarian Cancer															
IGROV1	16.3	18.5	16.2	4.93	14.2	38.4	34.6	34.4	17.7	29.8	90.4	64.9	73.0	45.0	62.4
OVCAR-3	20.4	28.9	20.9	6.88	15.0	60.1	96.5	73.2	19.7	29.4	>100	>100	>100	45.6	57.6
OVCAR-4	15.4	19.2	8.25	4.77	14.2	33.3	40.7	27.0	21.1	34.1	72.0	86.6	79.1	78.6	81.7
OVCAR-5	23.8	19.1	19.8	7.31	16.5	>100	44.2	45.5	20.9	33.1	>100	>100	>100	48.2	66.5
OVCAR-8	15.7	18.0	14.8	4.92	16.5	30.7	33.1	29.5	17.0	31.0	59.7	60.9	58.7	49.6	61.7
NCI/ADR-RES	14.9	---	---	---	13.3	30.0	----	---	---	29.1	60.7	---	---	---	63.7
SK-OV-3	15.8	17.3	13.7	10.6	14.2	33.9	34.1	33.2	23.6	28.6	72.6	67.2	89.2	52.4	57.8
Renal Cancer															
786-0	16.2	21.3	15.6	6.43	15.7	56.0	51.8	31.1	20.6	30.5	>100	>100	62.2	51.6	59.3
A498	14.5	16.8	17.8	16.8	16.3	30.9	32.1	35.3	31.2	30.7	65.8	61.2	69.9	57.9	57.9
ACHN	18.1	18.6	12.6	4.05	11.9	61.0	35.7	26.4	14.8	24.8	>100	68.3	55.1	39.2	51.7
CAKI-1	29.5	19.3	15.7	5.26	16.2	>100	43.2	35.0	18.6	37.6	>100	96.5	78.0	44.7	86.9
RXF 393	13.2	17.3	4.91	3.14	10.2	29.9	34.5	21.1	13.3	22.2	67.5	69.1	68.0	41.8	48.6
SN12C	17.0	18.3	19.6	4.46	13.7	36.7	35.6	>100	16.8	27.9	78.9	60.1	>100	42.1	56.7
TK-10	15.0	17.0	13.6	5.81	12.9	30.6	33.5	31.1	20.5	36.7	62.4	66.0	71.0	58.0	>100
UO-31	---	28.1	9.90	2.54	---	---	>100	>100	12.2	---	---	>100	>100	35.3	---
Prostate Cancer															
PC-3	12.0	16.2	8.38	3.18	6.37	28.0	31.6	24.2	15.2	22.0	65.1	61.7	62.4	57.3	60.0
DU-145	19.4	20.5	20.3	13.9	20.7	43.9	40.2	46.6	30.3	46.6	99.7	78.9	>100	66.0	>100
Breast Cancer															
MCF7	15.7	17.3	12.8	4.95	13.6	49.7	33.1	26.5	19.4	28.3	>100	63.1	55.1	50.9	58.8
MDA-MB-231/ATCC	---	18.3	16.4	4.52	---	---	34.2	33.8	16.9	---	---	63.6	69.6	41.9	---
HS 578T	12.6	19.3	14.4	3.22	12.8	40.9	47.8	44.9	18.6	40.1	>100	>100	>100	>100	>100
BT-549	12.2	14.6	5.86	3.02	5.22	28.2	29.7	21.0	13.1	18.1	65.0	60.3	56.0	40.2	44.7
T-47D	19.5	30.4	18.2	5.84	17.7	>100	>100	69.2	33.8	45.0	>100	>100	>100	>100	>100
MDA-MB-468	19.0	26.0	11.4	4.45	12.9	64.7	69.3	32.4	16.6	27.0	>100	>100	91.5	46.5	56.4

KM12, respectively and subpanel CNS cancer SF-295, SNB-19 and U251 with GI% = 87.14, 86.63 and 83.8 in addition to breast cancer subpanel lines MCF7, HS 578T and T-47D with GI% = 84.88, 91.85 and 88.96, respectively (Table 1). Compound **7f** showed selective activity against subpanel leukemia cells (3 cell lines from 6, 50.00%) with GI% = 98.14, 97.25 and 97.15 for CCRF-CEM, K-562 and RPMI-

8226 cell lines. **7f** showed GI% = 92.58, 87.03 and 97.82 against EKVX, NCI-H226 and NCI-H23 non-small cell lung cancer (NSCLC) cell lines. Furthermore, it showed activity against colon cancer cell line HCC-2998 (GI% = 93.72), CNS cancer cell lines SF-268 (GI% = 84.34) and SNB-19 (GI% = 92.01), melanoma cell line SK-MEL-5 (GI% = 99.63), ovarian cancer cell lines OVCAR-4 (GI% = 99.35) and NCI/ADR-RES (GI% = 89.49), renal cancer cell lines CAKI-1 (GI% = 90.36), TK-10 (GI% = 87.89 and UO-31 (GI% = 93.62), and breast cancer MCF7 (GI% = 92.77) and T-47D (GI% = 98.19) (Table 1).

3.2.2. Five dose full NCI 60 cell panel assay.

According to the promising data of compounds **7b-f** in the preliminary screening (1 dose, 10 μM), they were selected for further assessment at 5 doses concentrations (0.01, 0.1, 1, 10, 100 μM). The calculated response parameters: GI_{50}, TGI and LC_{50} of **7b-f** against the 60 cell lines are shown in Table 2. GI_{50} indicates the concentration that causes 50% decrease in the net cell growth, TGI (Total Growth Inhibition) represents cytostatic activity, while LC_{50} (Lethal dose) represents the concentration that causes 50% loss of the initial cells [49]. Compounds **7b-f** showed marked anticancer activity against most of tested cell lines with GI_{50} range 6.05-49.70, 14.60-53.20, 2.99-38.70, 2.47-16.80 and 3.40-20.70 μM, respectively (Table 2). Compounds **7b-f** revealed noticeable cytostatic activity (TGI) (Table 2) and they revealed LC_{50} values >100 μM against 29, 24, 20, 8 and 8 of the full panel tested cell lines, respectively which reflected their non-lethal effects. Also, reasonable LC_{50} values in the range 51.4-99.7, 55.4-96.5, 51.50-98.70, 33.20-92.40 and 41.5-86.90 μM for the remaining cell lines of the full panel, which reflected their moderate lethal effects (Table 2).

Subpanel and full panel mean graph midpoints (MG-MID) were calculated for the obtained GI_{50} values to indicate the average activity over the subpanels and full panel cell lines (Table 3). Compounds **7b-f** exhibited the mean average for 9 subpanels GI_{50} (MG-MID) in the range of 15.70-23.01, 17.57-42.24, 8.79-15.61, 3.61-8.86, 8.32-14.84 μM, respectively, and mean average of GI_{50} for full panel MG-MID = 18.11, 22.93, 13.19, 6.04, 12.20 μM, respectively (Table 3).

Moreover, the selectivity index (SI) which expresses the compound selectivity towards the subpanels was calculated by dividing the compound full panel MG-MID (μM) by its subpanel MG-MID (μM). Generally, compounds **7b-f** showed non-selective broad-spectrum anticancer activity towards cancer subpanels, with SI range 0.79-1.15, 0.50-1.25, 0.84-1.50, 0.68-1.42 and 0.82-1.47, respectively (Table 3).

3.2.3. SAR studies

The previous potent anticancer results of compounds **7a-f** revealed the impact of the electronic characteristics of the indoline moiety with respect to the substituents in positions 1 and 5 where the *N*-substituted indolines in **6a-f** produced less anticancer activity compared to the *N*-unsubstituted ones **7a-f** (Figure 3). The halogen substitution with chlorine or bromine atom in position 5 of the indoline moiety in **7b**, **7c**, **7e** and **7**f enhanced their anticancer activity (Figure 3). On the other hand, the replacement of the aryl group in **6a-f** by a five membered heterocyclic ring such as furan or thiophene in position 6 of the pyrazolo[3,4-*b*]pyridine system exhibited pronounced anticancer activity for **7a-f** against most of the tested cell lines (Figure 3). Thiophene ring in **7d** increased the anticancer activity when compared with the furan derivative **7a** (Figure 3).

Table 3. MG-MID (Mean Growth) of GI_{50} (uM) of subpanel and full panel tumor cell lines, and SI (Selectivity Index).

Cell line/Compound	7b		7c		7d		7e		7f	
	MG-MID	SI	MG-MID	SI	MG-MID	SI	MG-MID	SI	MG-MID	SI
Leukemia	21.56	0.84	42.24	0.50	8.79	1.50	4.25	1.42	8.32	1.47
Non-Small Cell Lung Cancer	16.97	1.07	21.97	1.04	13.86	0.95	6.09	0.99	11.18	1.09
Colon Cancer	23.01	0.79	25.73	0.89	11.29	1.17	6.02	1.00	11.62	1.05
CNS Cancer	16.66	1.09	19.52	1.17	11.81	1.12	3.61	1.67	9.43	1.29
Melanoma	18.15	1.00	18.73	1.22	15.48	0.85	8.86	0.68	14.61	0.84
Ovarian Cancer	17.47	1.04	20.17	1.14	15.61	0.84	6.57	0.92	14.84	0.82
Renal Cancer	17.64	1.03	19.59	1.17	13.71	0.96	6.06	1.00	13.84	0.88
Prostate Cancer	15.70	1.15	18.35	1.25	14.34	0.92	8.54	0.71	13.54	0.90
Breast Cancer	15.80	1.15	20.09	1.04	13.81	0.96	4.33	1.39	12.44	0.98
Full panel MG-MID	18.11 (μM)		22.93 (μM)		13.19 (μM)		6.04 (μM)		12.20 (μM)	

MG-MID = The average activity parameter over each subpanel.
Full panel MG-MID = The average activity over full panel.
SI (Selectivity Index) = The dividing the full panel MG-MID (μM) by subpanel MG-MID (μM) for each compound.

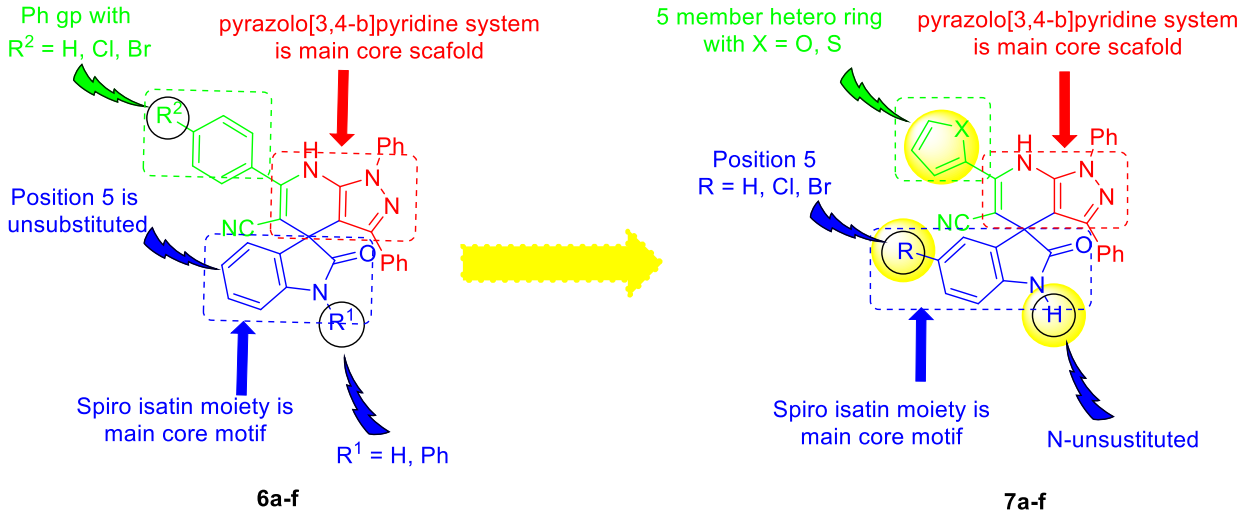

Figure 3. Structure features of potent anticancer agents **7a-f** compared with **6a-f**.

*3.2.4. Cytotoxicity of compounds **7b-f** on normal cell line WI-38*

The cytotoxicity of compounds **7b-f** towards normal cell line WI-38 was evaluated using MTT assay compared to nutlin-1 as reference compound. The safety profile of the tested compounds is expressed in cytotoxic concentration (IC_{50} in µM) (Table 4). Compounds **7b** (IC_{50} = 29.91 ± 4.70 µM), **17c** (IC_{50} = 49.39 ± 4.59 µM), **7d** (IC_{50} = 59.34 ± 4.54 µM), **7e** (IC_{50} = 34.82 ± 3.87 µM) and **7f** (IC_{50} = 58.69 ± 7.15 µM) showed acceptable cytotoxicity profiles on normal cell line WI-38 when compared with nutlin-1 (IC_{50} = 44.73 ± 6.61 µM) (Table 4).

Table 4. *In vitro* anti-proliferative activities of the tested compounds against human normal WI-38 cells (all treated for 72 h).

Compound	*In vitro* cytotoxicity IC_{50} (µM)[a]
7b	29.91 ± 4.70
7c	49.39 ± 4.59
7d	59.34 ± 4.54
7e	34.82 ± 3.87
7f	58.69 ± 7.15
Nutlin-1	44.73 ± 6.61

*3.2.5. In vitro inhibitory activity for **7b-f** on p53-MDM2 protein-protein interaction:*

The inhibitory activity of compounds **7b-f** on p53-MDM2 protein-protein interaction was assessed in MCF7 cell line using nutlin-1 as reference compound and the IC_{50} values and folds of activity compared to nutlin-1 are presented in Table 5.

Table 5. IC_{50} (µM) of p53-MDM2 protein-protein interaction inhibitory activity for **7b-f** and **nutlin-1** in MCF7 cell line

Compound	p53-MDM2 protein-protein interaction IC_{50} (µM)	Folds
7b	6.39± 0.22	1.28
7c	26.93± 1.11	0.30
7d	15.14± 0.57	0.54
7e	6.11± 0.22	1.34
7f	3.05± 0.12	2.69
Nutlin-1	8.21± 0.25	1.00

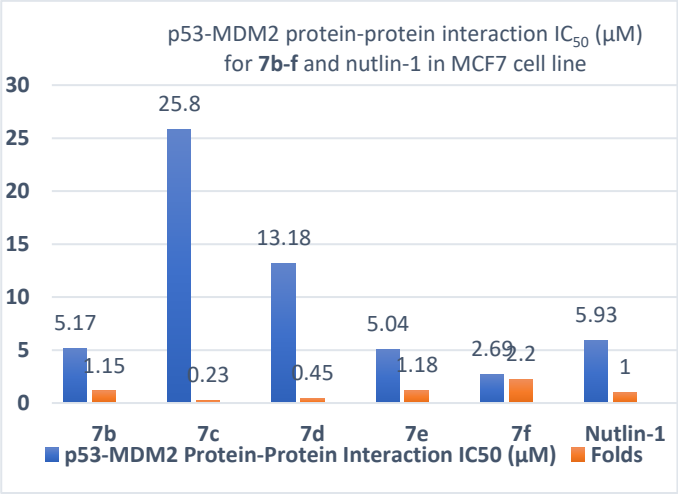

Figure 4. p53-MDM2 protein-protein interaction IC_{50} (µM) and folds comparison for **7b-f** and **nutlin-1** in MCF7 cell line.

The results revealed that compound **7f** was the most potent compound with IC_{50} = 3.05 ± 0.12 µM and 2.7-folds when compared with nutlin-1 (IC_{50} = 8.21 ±

0.25 µM) (Table 5 and Figure 4). Compounds **7b** and **7e** showed good inhibition of p53-MDM2 protein-protein interaction with IC_{50} = 6.39 ± 0.22 and 6.11± 0.22 µM, respectively, when compared with nutlin-1 (8.21 ± 0.25 µM) with 1.28- and 1.34-folds, respectively (Table 5 and Figure 4). Compounds **7c** and **7d** exhibited IC_{50} = 26.93 ± 1.11 and 15.14 ± 0.57 µM, respectively with 0.30 and 0.54 folds the activity of nutlin-1 (Table 5 and Figure 4).

*3.2.6. Effect of compounds **7b-f** on p53* in HepG2

Effect of the most active compounds **7b-f** and nutlin-1 as standard reference on p53 in HepG2 cell line was evaluated. Compounds **7b-f** and nutlin-1 were applied to the cell at conc. of 10 µM for 72 h. The values are given as fold changes from the control, which is set to 1 (Table 6 and Figure 5). When compared to nutlin-1, which demonstrated 12.10-folds and when compared to control HepG2, compounds **7b–f** displayed fold changes of 9.50, 2.89, 4.60, 0.86, and 0.71, respectively.

Table 6. The effect of **7b-f** and **nutlin-1** on the level of p53 in HepG2 cell line at 10 µM.

Compound	old change*
Control**	1.00
Nutlin-1	12.10
7b	9.50
7c	2.89
7d	4.60
7e	0.86
7f	0.71

***** The values are given as fold changes from the control
****Control = HepG2 cell line

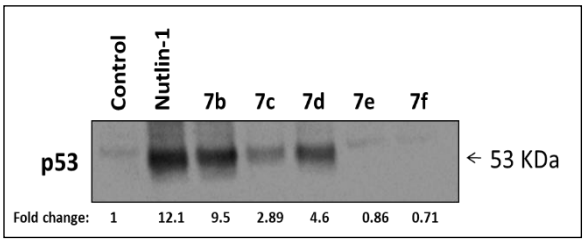

Figure 5. Effect of **7b-f** and **nutlin-1** on the level of p53 in HepG2 cell line at 10 µM

*3.2.7. Effect of compounds **7b**, **7e** and **7f** on the level of p21 and p53 in MOLT4 and HOP92 cells*

The inhibition of the p53-MDM2 interaction results in increasing of p53 level and increasing the level of its targeted gene p21 protein. Subsequently, the levels of p53 and p21 in leukemia MOLT4 cancer cells treated with **7b** and in cancer cells of non-small cell lung cancer HOP92 treated with **7e** or **7f** were evaluated. Compound **7b** increased the level of p53 by 3.86-folds in leukemia MOLT4 cancer cells whereas **7e** and **7f** increased the level of p53 by 2.53- and 2.98-folds in cancer cells of non-small cell lung cancer HOP92, respectively (Table 7 and Figure 6).

Table 7. Effect of **7b, e, f** on the level of p53 in MOLT4 and HOP92 cells.

Comp / Cell	p53 (ng/ml)	Folds*
7b / MOLT4	0.899	3.86
Cont. MOLT4	0.233	1
7e / HOP92	0.700	2.15
7f / HOP92	0.970	2.98
Cont. HOP 92	0.325	1

***** The values are given as fold changes from the control

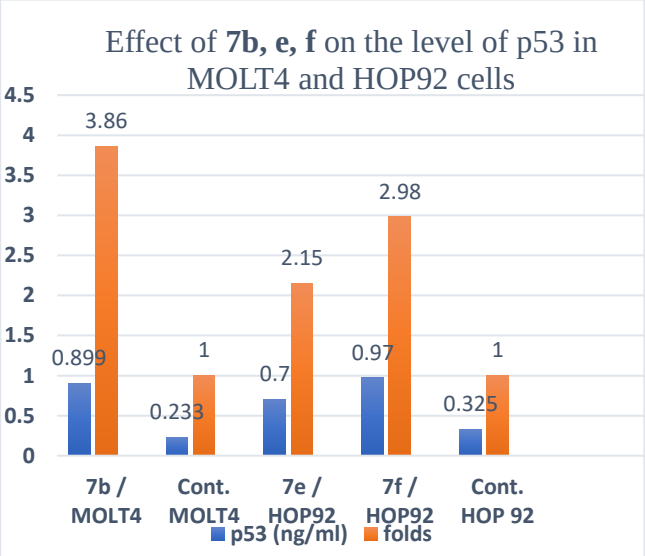

Figure 6. Effect of **7b, e, f** on the level of p53 in MOLT4 and HOP92 cells.

In addition, compound **7b** raised the level of p21 by 1.78-folds in leukemia MOLT4 cancer cells whereas **7e** and **7f** increased the level of p21 by 2.74- and 2.43-folds in cancer cells of non-small cell lung cancer HOP92, respectively (Table 8 and Figure 7).

Table 8. The effect of **7b, e, f** on the level of p21 in MOLT4 and HOP92 cells.

Comp / Cell	p21 (ng/ml)	Folds*
7b / MOLT4	0.184	1.78
Cont. MOLT4	0.103	1
7e / HOP92	0.220	2.74
7f / HOP92	0.195	2.43
Cont. HOP 92	0.080	1

***** The values are given as fold changes from the control

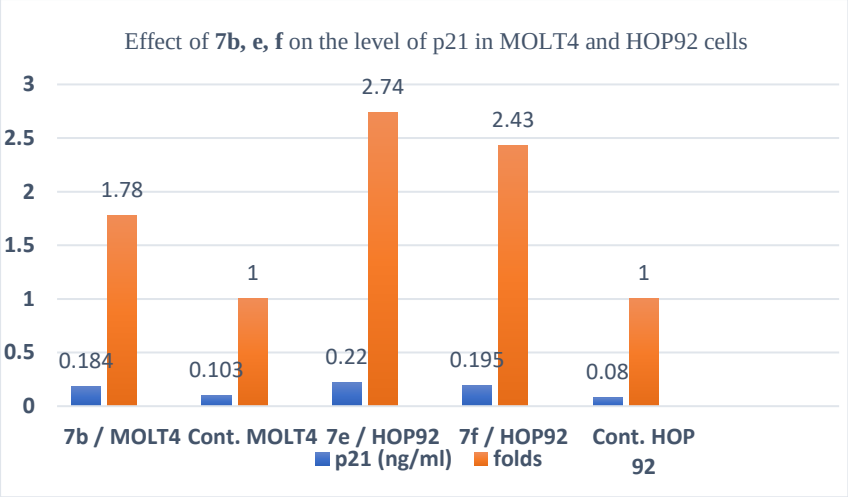

Figure 7. Effect of **7b, e, f** on the level of p21 in MOLT4 and HOP92 cells

*3.2.8. Apoptotic assay for compounds **7b**, **e**, **f***

Apoptotic assay using Annexin V/PI analysis for compounds **7b**, **7e** and **7f** revealed a significant level of early and late apoptosis on MCF7 in comparison with the control cells (Table 9, Figures 8 and 9). Compounds **7b**, **7e** and **7f** showed early apoptosis 29.06, 25.03 and 21.66 in MCF7 when compared with control MCF7 (0.42). In addition, compounds **7b**, **7e** and **7f** showed late apoptosis 19.23, 12.37 and 16.02 in MCF7 when compared with control MCF7 (0.27) (Table 9, Figures 8 and 9).

Table 9. Apoptosis analysis for **7b**, **7e** and **7f** against MCF7.

Compound	Apoptosis			Necrosis
	Total	Early	Late	
7b / MCF7	54.03	29.06	19.23	5.74
7e / MCF7	39.81	25.03	12.37	2.41
7f / MCF7	41.66	21.66	16.02	3.98
Control MCF7	2.25	0.42	0.27	1.56

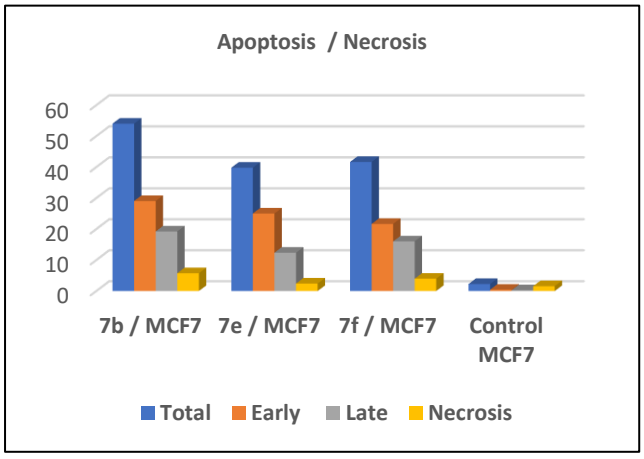

Figure 8. Apoptosis analysis for **7b**, **7e** and **7f** against MCF7.

3.3. Molecular modeling study

The co-crystallized ligand ((2'R,3R,4'R,5'R)-6-chloro-4'-(3-chloro-2-fluorophenyl)-2'-(2,2-dimethylpropyl)-*N*-(2-morpholin-4-ylethyl)-2-oxo-1,2-dihydrospiro[indole-3,3'-pyrrolidine]-5'-carboxamide) showed four binding interactions with Leu54, His96, Phe86 and Tyr67 amino acids (Figure 10a).

The investigated derivatives **7b**, **7e** and **7f** showed good binding interactions of -9.90, -10.34 and -10.15 kcal/mol., respectively compared to the co-crystallized ligand (-10.51 kcal/mol.). Compound **7b** exhibited interactions with Leu54 and Gly58 amino acids (Figure 10b). Additionally, compound **7e** revealed more binding interactions with Leu54, Phe55 and His96 amino acids (Figure 10c). Eventually, compound **7f** showed higher number of interactions with Leu54, Gly58, His96 and Ile99 residues (Figure 10d).

4. Conclusion

A facile and convenient synthesis of the target spiro-indoline-pyrazolo[3,4-*b*]pyridines **6a-f** and **7a-f** was achieved through three components-one-step synthesis. Compounds **7b-f** exhibited very promising activity in the 5-dose assay with full panel GI_{50} range 6.05-49.70, 14.60-53.20, 2.99-38.70, 2.47-16.80 and 3.40-20.70 µM, respectively, and GI_{50} (MG-MID) Full panel = 18.11, 22.93, 13.19, 6.04, 12.20 µM, respectively. *In vitro* p53-MDM2 binding assay showed that **7f** is the most potent compound with IC_{50} = 3.05 ± 0.12 µM and 2.7-folds when compared with nutlin-1 (IC_{50} = 8.21 ± 0.25 µM). Furthermore, compound **7b**, **7e** and **7f** increased the level of p53 and p21 in leukemia MOLT4 and non-small cell lung cancer HOP92. Compounds **7b**, **7e** and **7f** induced a significant level of apoptosis on MCF7. Molecular docking studies revealed that compounds **7b**, **7e** and **7f** interacted with the p53 cleft on MDM2 with good binding mode.

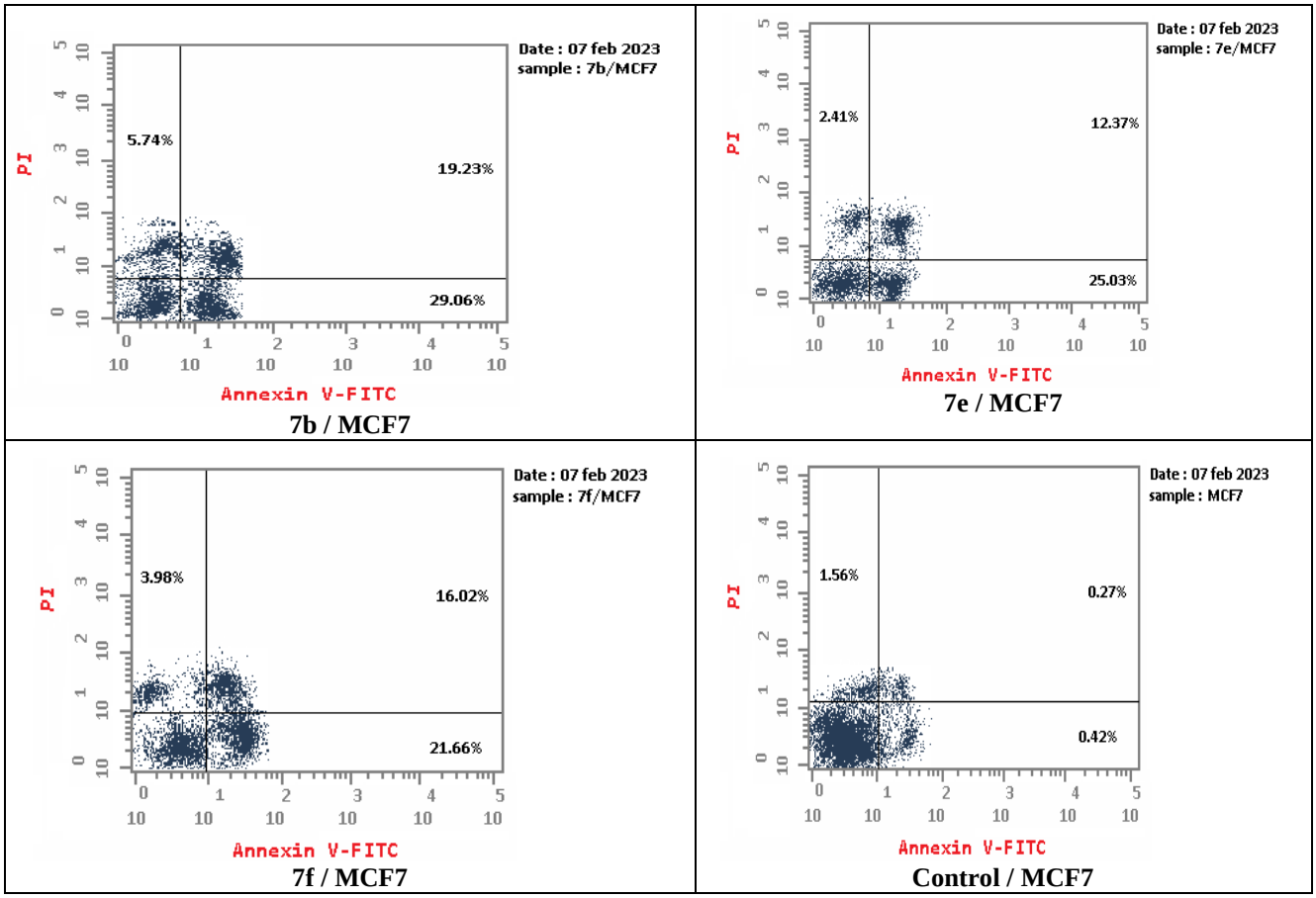

Figure 9. Apoptotic analysis for compounds **7b, 7e** and **7f** against MCF7

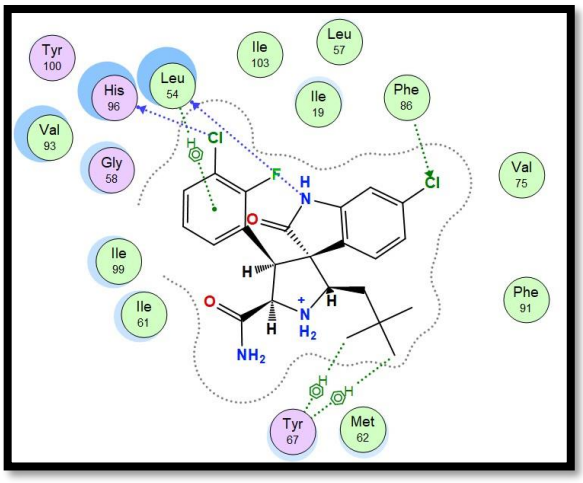

Figure 10a. 2D interactions of the co-crystallized ligand with MDM2 active site

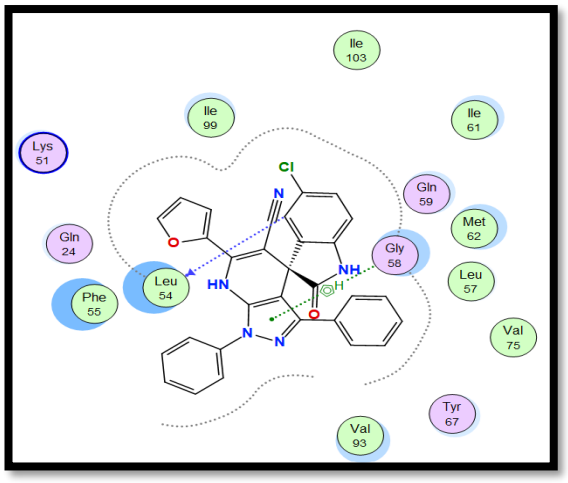

Figure 10b. 2D interactions of compound **7b** with MDM2 active site

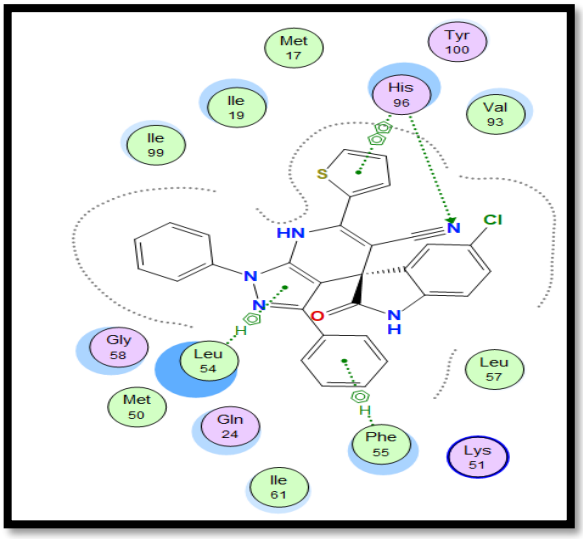

Figure 10c: 2D interactions of compound **7e** with MDM2 active site

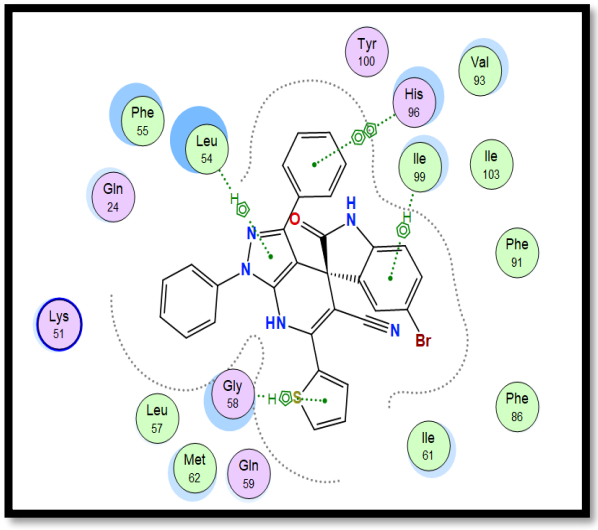

Figure 10d: 2D interactions of compound **7f** with MDM2 active site

Figure 10. 2D interactions of the co-crystallized ligand with MDM2 active site, **7b**, **7e** and **7f**.

5. Conflict of interest:

The authors declare that they have no conflict of interest

6. References

[1] A.K. Gupta, M. Bharadwaj, A. Kumar, R. Mehrotra, "Spiro-oxindoles as a Promising Class of Small Molecule Inhibitors of p53-MDM2 Interaction Useful in Targeted Cancer Therapy", Topics curr. chem., (2017), 375(1), 3.

[2] L. Galluzzi, A. Buqué, O. Kepp, L. Zitvogel, G. Kroemer, "Immunological Effects of Conventional Chemotherapy and Targeted Anticancer Agents", Cancer Cell, (2015), 28(6), 690-714.

[3] K. Dzobo, D.A. Senthebane, C. Ganz, N.E. Thomford, A. Wonkam, C. Dandara, "Advances in Therapeutic Targeting of Cancer Stem Cells within the Tumor Microenvironment: An Updated Review" Cells, (2020), 9(8), 1896.

[4] S. Wang, Y. Zhao, A. Aguilar, D. Bernard, C.Y. Yang, "Targeting the MDM2-p53 Protein-Protein Interaction for New Cancer Therapy: Progress and Challenges", Cold Spring Harb. Perspect. Med., (2017), 7(5), a026245.

[5] T. Ozaki, A. Nakagawara, "Role of p53 in Cell Death and Human Cancers", Cancers, (2011), 3(1), 994-1013.

[6] J.T. Zilfou, S.W. Lowe, "Tumor suppressive functions of p53. Cold Spring Harb. Perspect. Biol. (2009), 1(5), a001883.

[7] D. Shi, W. Gu, "Dual Roles of MDM2 in the Regulation of p53: Ubiquitination Dependent and Ubiquitination Independent Mechanisms of MDM2 Repression of p53 Activity" Genes Cancer, (2012), 3(3-4), 240-248.

[8] S. Shangary, S. Wang, "Targeting the MDM2-p53 interaction for cancer therapy", Clin. Cancer Res. (2008), 14(17), 5318-5324

[9] J. Chen, "The Cell-Cycle Arrest and Apoptotic Functions of p53 in Tumor Initiation and Progression", Cold Spring Harb. Perspect. Med. (2016), 6(3), a026104.

[10] S. Shangary, S. Wang, "Small-molecule inhibitors of the MDM2-p53 protein-protein interaction to reactivate p53 function: a novel approach for cancer therapy", Annu. Rev. Pharmacol. Toxicol., (2009), 49, 223-241.

[11] S. Patel, M.R. Player, "Small-molecule inhibitors of the p53-HDM2 interaction for the treatment of cancer", Expert Opin. Investig. Drugs. (2008), 17(12), 1865-1882.

[12] P. Chène, "Inhibition of the p53-MDM2 interaction: targeting a protein-protein interface", Mol. Cancer Res. (2004), 2(1), 20-28.

[13] A. Lauria, M. Tutone, M. Ippolito, L. Pantano, A.M. Almerico, "Molecular modeling approaches in the discovery of new drugs for anti-cancer therapy: the investigation of p53-MDM2 interaction and its inhibition by small molecules", Curr. Med. Chem., (2010), 17(28), 3142-3154.

[14] K. Khoury, A. Dömling, "P53 mdm2 inhibitors", Curr. Pharm. Des., (2012), 18(30), 4668-4678.

[15] S. Nag, X. Zhang, K.S. Srivenugopal, M.H. Wang, W. Wang, R. Zhang, "Targeting MDM2-p53 interaction for cancer therapy: are we there yet?", Curr. Med. Chem., (2014), 21(5), 553-574.

[16] C. Klein, L.T. Vassilev, "Targeting the p53-MDM2 interaction to treat cancer", Br. J. Cancer. (2004), 91(8), 1415-1419.

[17] J.C. Carry, C. Garcia-Echeverria, "Inhibitors of the p53/hdm2 protein-protein interaction-path to the clinic", Bioorg. Med. Chem. Lett., (2013), 23(9), 2480-2485.

[18] Chène, P. 'Inhibiting the p53–MDM2 interaction: an important target for cancer therapy'. Nat Rev. Cancer, (2003), 3, 102-109.

[19] L.T. Vassilev, B.T. Vu, B. Graves, D. Carvajal, F. Podlaski, Z. Filipovic, N. Kong, U. Kammlott, C. Lukacs, C. Klein, N. Fotouhi, E.A. Liu, "In vivo activation of the p53 pathway by small-molecule antagonists of MDM2", Science. (2004), 303(5659), 844-848.

[20] E.K. Crane, S.Y. Kwan, D.I. Izaguirre, Y.T. Tsang, L.K. Mullany, Z. Zu, J.S. Richards, D.M. Gershenson, K.K. Wong, "Nutlin-3a: A Potential Therapeutic Opportunity for TP53 Wild-Type Ovarian Carcinomas", PLoS One. (2015), 10(8), e0135101.

[21] C. Tovar, B. Graves, K. Packman, Z. Filipovic, B. Higgins, M. Xia, C. Tardell, R. Garrido, E. Lee, K. Kolinsky, K.H. To, M. Linn, F. Podlaski, P. Wovkulich, B. Vu, L.T. Vassilev, "MDM2 small-molecule antagonist RG7112 activates p53 signaling and regresses human tumors in preclinical cancer models", Cancer Res. (2013), 73(8), 2587-2597.

[22] S. Trino, L. De Luca, I. Laurenzana, A. Caivano, L. Del Vecchio, G. Martinelli, P. Musto, "P53-MDM2 Pathway: Evidences for A New Targeted Therapeutic Approach in B-Acute Lymphoblastic Leukemia", Front. Pharmacol. (2016), 7, 491.

[23] M. Andreeff, K.R. Kelly, K. Yee, S. Assouline, R. Strair, L. Popplewell, *et. al.*, "Results of the phase I trial of RG7112, a small-molecule MDM2 antagonist in Leukemia. Clin. Cancer Res., (2016), 22, 868-876.

[24] Q. Ding, Z. Zhang, J.J. Liu, N. Jiang, J. Zhang, T.M. Ross, X.J. Chu, D. Bartkovitz, F. Podlaski, C. Janson, C. Tovar, Z.M. Filipovic, B. Higgins, K. Glenn, K. Packman, L.T. Vassilev, B. Graves, "Discovery of RG7388, a potent and selective p53-MDM2 inhibitor in clinical development", J. Med. Chem., (2013), 56(14), 5979-5983.

[25] X. Fan, Y. Wang, J. Song, H. Wu, M. Yang, L. Lu, X. Weng, L. Liu, G. Nie, "MDM2 inhibitor RG7388 potently inhibits tumors by activating p53 pathway in nasopharyngeal carcinoma", Cancer Biol. Ther., (2019), 20(10), 1328-1336.

[26] M. Zanjirband, R.J. Edmondson, J. Lunec, "Pre-clinical efficacy and synergistic potential of the MDM2-p53 antagonists, Nutlin-3 and RG7388, as single agents and in combined treatment with cisplatin in ovarian cancer", Oncotarget. (2016), 7(26), 40115-40134.

[27] M. Espadinha, E.A. Lopes, V. Marques, J.D. Amaral, D.J.V.A. dos Santos, M. Mori, S. Daniele, R. Piccarducci, E. Zappelli, C. Martini, C. M.P. Rodrigues, M.M.M. Santos, "Discovery of MDM2-p53 and MDM4-p53 protein-protein interactions small molecule dual inhibitors", Eur. J. Med. Chem., (2022), 241, 114637.

[28] Z. Zhang, Q. Ding, J.J. Liu, J. Zhang, N. Jiang, X.J. Chu, D. Bartkovitz, K.C. Luk, C. Janson, C. Tovar, Z.M. Filipovic, B. Higgins, K. Glenn, K. Packman, L.T. Vassilev, B. Graves, "Discovery of potent and selective spiroindolinone MDM2 inhibitor, RO8994, for cancer therapy", Bioorg. Med. Chem., (2014), 22(15), 4001-4009.

[29] A. Aguilar, W. Sun, L. Liu, J. Lu, D. McEachern, D. Bernard, J.R. Deschamps, S. Wang, "Design of chemically stable, potent, and efficacious MDM2 inhibitors that exploit the retro-mannich ring-opening-cyclization reaction mechanism in spiro-oxindoles", J. Med. Chem. (2014), 57(24), 10486-10498.

[30] J.A. Canner, M. Sobo, S. Ball, B. Hutzen, S. DeAngelis, W. Willis, A.W. Studebaker, J. Ding, S. Wang, D. Yang, J. Lin, "MI-63: a novel small-molecule inhibitor targets MDM2 and induces apoptosis in embryonal and alveolar rhabdomyosarcoma cells with wild-type p53", Br J Cancer., (2009), 101(5), 774-81.

[31] M. Zheng, J. Yang, X. Xu, J. T. Sebolt, S. Wang, Y. Sun, "Efficacy of MDM2 inhibitor MI-219 against lung cancer cells alone or in combination with MDM2 knockdown, a XIAP inhibitor or etoposide", Anticancer Res. (2010), 30(9), 3321-3331.

[32] J. Lu, D. McEachern, S. Li, M. J. Ellis, S. Wang, "Reactivation of p53 by MDM2 Inhibitor MI-77301 for the Treatment of Endocrine-Resistant Breast Cancer", Mol. Cancer Ther., (2016), 15(12), 2887-2893.

[33] Y. Zhao, S. Yu, W. Sun, L. Liu, J. Lu, D. McEachern, S. Shargary, D. Bernard, X. Li, T. Zhao, P. Zou, D. Sun, S. Wang, "A potent small-molecule inhibitor of the MDM2-p53 interaction (MI-888) achieved complete and durable tumor regression in mice", J. Med. Chem. (2013), 56(13), 5553-5561.

[34] H.S. Ibrahim, W.M. Eldehna, A.L. Fallacara, E.R. Ahmed, H.A. Ghabbour, M.M. Elaasser, M. Botta, S.M. Abou-Seri, H.A. Abdel-Aziz, "One-pot synthesis of spiro(indoline-3,4'-pyrazolo[3,4-b]pyridine)-5'-carbonitriles as p53-MDM2 interaction inhibitors", Future Med. Chem. (2018), 10(24), 2771-2789.

[35] W.M. Eldehna, D.H. El-Naggar, A.R. Hamed, H.S. Ibrahim, H.A. Ghabbour, H.A. Abdel-Aziz, "One-pot three-component synthesis of novel spirooxindoles with potential cytotoxic activity against triple-negative breast cancer MDA-MB-231 cells", J Enzyme Inhib Med Chem., (2018), 33(1), 309-318.

[36] A.A. Esmaili, A. Bodaghi, "New and efficient one-pot synthesis of functionalized γ-spirolactones mediated by vinyltriphenylphosphonium salts" Tetrahedron, (2003), 59(8), 1169-1171.

[37] M. S. Shmidt, A. M. Reverdito, L, Kremenchuzky, I. A. Perillo, M. M. Blanco, "Simple and efficient microwave assisted N-alkylation of isatin", Molecules, (2008), 13(4), 831-840.

[38] L. Ma, L. Yuan, C. Xu, G. Li, M. Tao, W. Zhang, "An Efficient Synthesis of 2-Aminothiophenes via the Gewald Reaction Catalyzed by an N-Methylpiperazine-Functionalized Polyacrylonitrile Fiber", Synthesis, (2013), 45, 45-52.

[39] W.-N. Su, T.-P. Lin, K.-M. Cheng, K.-C. Sung, S.-K. Lin, F.F. Wong, "An efficient one-pot synthesis of N-(1,3-diphenyl-1H-pyrazol- 5-yl)amides", J. Heterocycl. Chem. (2010), 47, 831–837.

[40] A. Monks, D. Scudiero, P. Skehan, R. Shoemaker, K. Paull, D. Vistica, C. Hose, J. Langley, P. Cronise, A. Vaigro-Wolff, M. Gray-Goodrich, H. Campbell, J. Mayo, M. Boyd "Feasibility of a high-flux anticancer drug screen using a diverse panel of cultured human tumor cell lines", J. Nat. Cancer Inst., (1991), 83, 757–766.

[41] M.R. Boyd, K.D. Paull, "Some practical considerations and applications of the national cancer institute in vitro anticancer drug discovery screen", Drug Develop. Res., (1995), 34, 91-109.

[42] E.A. Orellana, A.L. Kasinski, "Sulforhodamine B (SRB) Assay in Cell Culture to Investigate Cell Proliferation", Bio-Protoc., (2016), 61.

[43] J.M. Edmondson, L.S. Armstrong, A.O. Martinez, "A rapid and simple MTT-based spectrophotometric assay for determining drug sensitivity in monolayer cultures", J. Tissue Cult. Methods, (1988), 11, 15-17.

[44] P. Pozarowski, Z. Darzynkiewicz, "Analysis of cell cycle by flow cytometry", Methods Mol. Biol., (2004), 281, 301-311.

[45] L.C. Crowley, A.P. Scott, B.J. Marfell, J.A. Boughaba, G. Chojnowski, N.J. Waterhouse, "Measuring Cell Death by Propidium Iodide Uptake and Flow Cytometry", Cold Spring Harb. Protoc., (2016), 2016, 647.

[46] G.M. Popowicz, A. Czarna, S. Wolf, K. Wang, W. Wang, A. Dömling, T.A. Holak, "Structures of low molecular weight inhibitors bound to MDMX and MDM2 reveal new approaches for p53-MDMX/MDM2 antagonist drug discovery" Cell cycle, (2010), 9(6), 1104-1111

[47] X. Gao, Z. Yang, W. J. Hao, B. Jiang, S. J. Tu, "Three-component synthesis of spiro [indoline-3, 4'-pyrazolo[3,4-b]pyridines] under microwave irradiation", J. Heterocycl. Chem. (2017), 54(4), 2434-2439.

[48] T. Chen, X. P. Xu, S.J. Ji, "Novel, one-pot, three-component route to indol-3-yl substituted spirooxindole derivatives", J. Comb. Chem. (2010), 12(5), 659-663.

[49] E.Z. Mohammed, W.R. Mahmoud, R.F. George, G.S. Hassan, F.A. Omar, H.H. Georgey, "Synthesis, in vitro anticancer activity and in silico studies of certain pyrazole-based derivatives as potential inhibitors of cyclin dependent kinases (CDKs)", Bioorg. Chem., (2021), 116, 105347.